Master Thesis Final Work

Control of Renewable Distributed Energy Sources in Microgrids

$\boldsymbol{September\ 22^{nd}, 2020}$

Author: *Giulio Colnago*

Director: *Eduardo Prieto Araujo*

Escola Tècnica Superior d'Enginyeria Industrial de Barcelona

Abstract

This thesis studies and designs a microgrid with the following characteristics: alternative current, low voltage and grid-connected, features photovoltaic power generation, a suitable storage system and dynamic loads, able to manage zero-net metering with the main grid to which is interfaced.

This project also discusses main components of the microgrid providing theoretical principles on how it is modelled using software MATLAB/Simulink, showing graphical results of main simulations operated throughout the work.

Particular focus has been given to describe main control techniques of the power electronic devices needed in the model. A suitable control system for each component object of the study is provided for the correct operation of the microgrid.

Content

1. Table of Figures

2. Preface

Today, in modern large interconnected power grids, the need for integrating new technologies (such as renewable energy sources and energy storage) has also led to a search for new technological solutions and, for being one of the most promising, modern microgrids have emerged.

Although their concept was not mainstream in the first decade of the century, the technological progress and sudden surge of power electronics application in power systems have enabled microgrids expansion to the energy sector, opening for the endless opportunities and advantages that these new approaches to electricity distribution offer.

A microgrid not only provides backup for the main power system to which is connected improving its resilience, but can also be used to cut costs, connect to a local resource that is too small or unreliable for traditional grid use enhancing long-term energy security. A microgrid allows communities to be more energy independent and, in some cases, when integrating renewable generation, it results particularly environmentally friendly.

Furthermore, for their ability to function autonomously as physical or economic conditions dictate, especially in the developing world, the technology has enormous potential to provide a small-scale, self-contained electricity supply to remote areas where connection to the centralized grid can be arduous.

But said this, many operational challenges remain yet to be solved, as assumptions typically applied to conventional distribution systems are no longer valid.

Being quite different from bulk power network, low-inertia characteristic, intermittencies, complications in protection coordination and system-balancing problems are inherent in microgrids (especially in high-renewables').

But as these barriers can be overcome and addressed, for instance with careful control design or with storage and other proper technologies, integrating renewable energy into this power systems will become a practice of milestone importance for the sector and it is expected to drive the next growth phase for their development.

2.1 Motivation

This thesis project was born thanks to my great interest to the field of renewable energies. Even though my bachelor background is in Mechanical Engineering, over the years of my personal life and student career, I have always been keen on supporting environmental causes and grown more and more concerned about environmental issues.

At the same time, I became aware on the endless opportunities offered by renewables technologies, that while helping cutting carbon emissions and to mitigating climate change, will turn from being an alternative solution to being a staple of the energy sector in decades to come.

And it is for this interest and drive I felt back then that, in June 2018, I decided to join the InnoEnergy European Masters and, after two years as part of the RENE program, I can say I am more than ever captivated by this world.

Last year in Lisbon, attending a course on photovoltaic energy, I had the chance to widely broaden my knowledge on this technology while working on major projects regarding, for instance, the sizing of a power plant and its main basic control schemes.

Another compelling experience has been working, as part of a group of six friends and colleagues, on a year-long project for Esade Business School in Barcelona, that aimed at facing and solving droughts issues in the municipality of Cape Town, through the development and hypothetical implementation of a desalination plant run entirely with photovoltaic electricity.

From then on, I was able to deepen about other topics of fundamental importance for the energy sector, such as Energy Storage and Wind Power, that helped me to shape more and more the idea on what I would have eventually chosen as my TFM topic.

And as the result of the author involvement in other relevant project during last semester in UPC, final choice was to work on something related to the distribution of the energy obtained from renewable distributed energy sources, having fully understood why main challenges of the decarbonization of the energy sector are in fact due to the introduction of this collected energy into the main grid.

Hence, among the topics listed for possible thesis projects, when I first discussed with Professor Eduardo Prieto about developing something that would focus on the alternative current microgrid control framework, I did not hesitate to take on the work.

As the topic was almost completely unknown to the author before the first semester spent at UPC, this choice represented more than a challenge but at the same time an opportunity to learn more about a field that would be of milestone importance for the whole energy industry, as distributed generation and renewables not only offer a non-pollutant, cheap and efficient source of energy but also enhance the reliability of supply and reduce the need for additional power grid reinforcements.

As partially already said, previous knowledge required covered a wide range of subjects from basic electrical engineering and power systems to power electronics, dynamical systems and proportional integral controllers, energy storage and photovoltaic and wind power. A good command of MATLAB/Simulink software package was also required to develop all the components of the final microgrid model discussed and tested throughout this paper.

This project has helped to greatly enhance my knowledge on wind and photovoltaic energy integration to power systems and on the general functioning of electronic power devices related to it.

2.2 Objectives and scope

Microgrids (MGs), as it will be widely discussed in this paper, are good candidate to improve the existing electrical systems. However, the implications of including this kind of systems are complex. The main objective of this thesis is to study and comprehend them and to provide a control system for the operation of alternative currents (AC) MGs as grid-tied systems.

Relevant objectives are described in this chapter from more broad to detailed ones: design a MG for a grid-connected, Zero-Energy Community (ZEC), with a Low Voltage Direct Current (LVDC) distribution system and

a photovoltaic (PV) and wind powered distributed generation (DG) to be coupled with a suitable energy storage system (ESS).

In Scope:

- Design the general structure of the MG
- Identify the components of the MG
- Describe qualitatively main control techniques for MGs
- Describe the electronic power devices necessary for the correct operation of the MG
- Simulate the average model of the converter
- Model all the components of the MG
- Simulation of the whole electrical system having interaction between the all the different components
- Evaluate the environmental impact of the system

Out of scope:

- Simulation of the MG over a long time (simulation has been done for a $2\ s$ period)
- Description Pulse Width Modulation (PWM) technique to control the converters (only qualitatively)
- Considering commutation losses or converter efficiencies
- Doing an accurate study of the electrical demand of the loads
- Analyzing accurately cost of the described system (only a feasibility study has been done)
- Placing the MG in a real geographical area or test it applied to a real case scenario

3. Introduction

3.1 Microgrids

Nowadays the electrical energy sector is currently found in dramatic changing paradigm, which moves towards an increasing trend in generating power at distributions levels, where electricity is typically consumed, by means of non-conventional/renewable based generation units.

These new generation technologies, termed as distributed generation (DG), not only offers a non-pollutant, cheap and efficient source of energy to cover increasing demand, but also enhance the reliability of supply to critical loads and reduce the need for additional grid reinforcements (Cantarellas, Jan. 2018).

For many decades small scale autonomous grids have existed wherever connection to the main power grid is now feasible due to economical and/or technical difficulties (Chris Marnay, 2015).

MGs are decentralized electricity distribution systems containing loads and distributed energy sources that can be operated in a controlled, coordinated way whether they are (Chris Marnay, 2015):

- Local energy communities, not designed to operate in islanded mode and that consist in a number of consumers organized to benefit from distributed local energy production within a defined area to satisfy their needs
- Embedded MGs, privately owned and managed electricity infrastructure controllable whether in islanded mode or connected to the main grid system
- Isolated MGs, where, as already said, due to the lack of possibility of connection to the main power system because of economic issues or geographical position, the MGs only function in islanded mode

So that such systems, comprising low voltage (LV) systems with storage devices and flexible loads, can be found in airports, university and hospital campuses or in large commercial, industrial and military facilities (Chris Marnay, 2015).

Due to their scalability, competitive costs and flexibility in operating fossil-fuel based generation has always been the main choice for a source of electricity in powering, for instance, isolated areas or autonomous systems (Adam Hirscha, 2018).

But renewables have progressed at an unprecedented pace over the past decade thanks to technological advances, proved economic feasibility and competitiveness due to sharp cost reduction and effective policies and planning (including feed-in tariffs, tradable green certificates, renewable portfolio standards, etc.) couple with ambitious goals (Müller, 2018).

So that the integration in MGs of greener energy generation based on solar, wind, hydrogen and hydro power has become now a trend and a priority making MGs the near future candidate to reduce the dependence on the carbon-based generation, towards a more environmentally friendly and sustainable energy paradigm (Adam Hirscha Y. P., 2018).

MGs can help to delay investments on new electric infrastructures becoming a new entity to support classical power systems since opportunities like peak shaving capacity, energy optimization, voltage regulation, local market values, aggregation energy exchanges, smart-metering and pricing among others can be introduced (Adam Hirscha, 2018).

Between all opportunities and benefits just listed, main one is of environmental nature with Green House Gases (GHG) reduction. Distributed energy sources (DER) that are decentralized and flexible being located locally and generally in proximity to the small-scale load they serve, are of growing importance to address such issues nowadays (Adam Hirscha Y. P., 2018).

Renewable energy plays an important and growing role in the energy system of the European Union. The share of energy from renewable sources (RS) in gross final consumption of energy was 18% in 2018. This is double the share in 2004 with 8.5% (Marola, 2020).

The Europe 2020 strategy includes a target of reaching 20% of gross final energy consumption from RS by 2020, and at least 32% by 2030 (Commission).
These figures are based on energy use in all its forms across all three main sectors, the heating and cooling sector, the electricity sector and the transport sector.

But due to the irregularity of RS and their intrinsic aleatory nature (think of sun irradiance or wind speed for instance), MGs require special storage systems to store energy and give it to the system when required. This improves security of supply and lower the environmental impact on the whole but at the same time it adds complexity and costs for further implementation in the energy sector.

Furthermore, this unpredictability of the generated power would introduce large disturbances into the electric system, making it difficult to control, and eventually resulting in an unstable system.

So that, in order to allow a wide and successful integration of DER into LV and decentralized systems many technical challenges must yet be overcome to ensure that the levels of reliability are not significantly affected, and the potential benefits are fully harnessed (AL-Sunni, 2015).

In this sense, the further and main issues include:

- Schedule and dispatch of units under supply and demand uncertainty and determination of appropriate levels of reserves
- Reliable and economical operation of MGs with high penetration levels of intermittent generation in stand-alone mode of operation
- Design of appropriate Demand Side Management (DSM) schemes to allow customers to react to the grid's needs new market models that allow competitive participation of intermittent energy sources
- Reengineering of the protection schemes at the distribution level to account for bidirectional power flows

And currently main effort is being put on the development of new voltage and frequency control techniques to account for the increase in power-electronics-interfaced DG and that exhibit plug-and-play features to ensure reliable, secure and economical operation of MGs in either grid-connected or stand-alone mode (AL-Sunni, 2015).

This particular project focuses on developing and modelling a renewables-run AC MG and propose control techniques and strategy for a reliable operation of it and of each of its components.

All topics discussed in this introduction are addressed from a control point of view, that is, to tackle the electrical problems that could arise during the simulation of this to improve the overall performance of the system. Software used exclusively include MATLAB/Simulink.

The rest of the document is organized as follows:

Chapter 4 discusses the concept of MG control state, reviews the state-of-the art in MG primary control. After identifying the actors that play a key role in a LV grid, it is disclosed that the converter becomes a key element and the control of this becomes crucial.

In Chapter 5 the electrical system is briefly discussed. After this, based on the instantaneous power and linear control theories, the average model of Voltage Source Converter (VSC) is modelled along its main blocks (internal current control, power regulation outer loop, etc.) and final graphic results of two different DC generation scenarios are obtained.

In Chapter 6 all the other components of the MG are introduced and modelled: a PV generator (PV array and MPPT DC/DC converter), a wind power generator (wind turbine based on a DFIG generator plus a back-to-back AC/DC/AC converter) and a battery storage system.

In chapter 7 main simulation of the final model of the grid is performed and graphic results are showed to exemplify the described control approach and to illustrate the dynamic performance of the control schemes implemented. Real and reactive power generated within the MG, including the temporary power transfer from/to storage units, is shown in balance with the shifting demand of local loads.

In chapter 8 some conclusions are drawn, potential environmental impact of such project is estimated and budget of the thesis work is showed.

4. State of the Art of Control

The MG can be seen as a LV neighborhood of the power system only to the extent that its behavior at the connection with this is maintained within the rigorous requirements of the grid. But at the same time, it should appear as an autonomous power system which meets the requirements of the customer. Voltage, reliability performance, and quality of power should be those that support the customers' objectives.

From a control perspective, techniques need to be developed which significantly lower the system complexity encountered with the addition of extra micro-sources to a MG. The presence of converter interfaces in fuel cells, PVs, microturbines and storage technologies creates a different situation when compared to more conventional synchronous generator sources in power sources and standby emergency power systems. Taking advantage of the properties of the power electronic interface to provide additional functionality to the MG and localized converter control technology, along with a minimal amount of short energy storage at the DC bus forms the basis for the approach.

Being self-commutated, the converter no longer relies on synchronous machines in the AC system for its operation. Various features of the converter control could include: plug-and-play features, seamless connection and isolation from the electric grid, independent control of reactive and active power, ability to correct voltage sags and system imbalances are all critical for the creation of a MG.

The main variables used to control the operation of a MG are voltage, frequency, and active and reactive power. In grid connected mode the main role of the MG control is to accommodate the active and reactive power generated by the DER units, and the load demand. Reactive power injection by a DER unit can be used for power factor correction, reactive power supply, or voltage control at the corresponding Point of Connection (PC).

In stand-alone mode of operation, the MG operates as an independent entity. This mode of operation is significantly more challenging than the grid connected mode because the critical demand-supply equilibrium requires the implementation of accurate load sharing mechanisms to balance sudden active power mismatches. Power balance is ensured either directly by local controllers utilizing local measurements or by a central controller that communicates appropriate set points to local controllers of different DER units and controllable loads. The main objective of such a mechanism is to ensure that all units contribute to supplying the load in a pre-specified manner in order to avoid any mismatch in the output voltage's phase angle or

amplitude that could cause high circulating currents. With regard to the architecture of a power system's control, in literature two very distinctive opposite approaches can be identified: centralized and decentralized (Joan Rocabert, 2012).

In a centralized scheme, computation of references and control actions are sent to each local single unit forming the system therefore requiring coordinated and extensive communication between the central controller and these while in a decentralized layout every single unit has its own controller functioning based on local information and unaware of the whole system-wide variables. But an interconnected power system usually covers extended geographic areas, making the implementation of a fully centralized approach infeasible due to the extensive communication and computation needs.

At the same time a minimum level of communication is required due to the coupling between operations of each element of the system and this cannot be achieved by using only local variables. So that a compromised between the control architectures could be exemplified with a hierarchical control structure made up by up to three control levels: primary, secondary and tertiary (Joan Rocabert, 2012).

These differ from each other for the time frame they operate, the speed response and their different infrastructure requirements for communication. It can be noted that such architecture follows closely the one of the wider utility host grid since, although MGs are not necessarily as geographically extented, the high number of generations and load units coupled with stringent requirements of performance make them benefit from such structure.

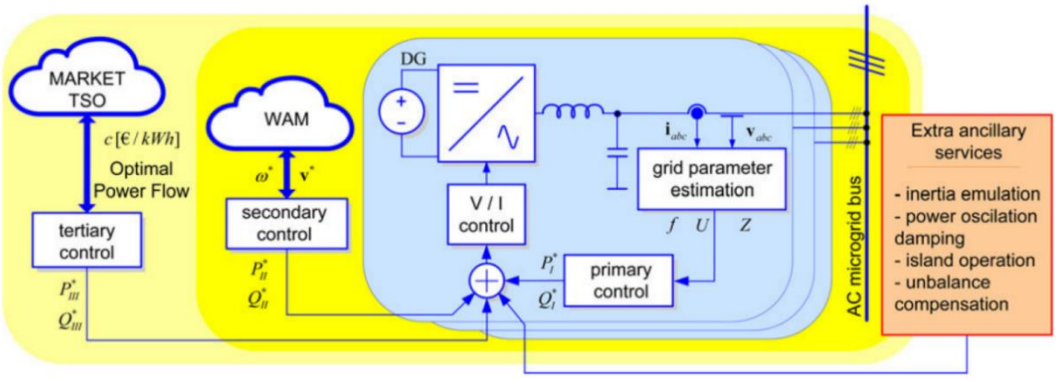

Fig. 1, Block diagram of primary secondary and tertiary MG control, from (Joan Rocabert, 2012)

Primary control is the first level in the control hierarchy, it features the promptest response and it is based exclusively on local measurements requiring no communication links, thus achieving a decentralized solution for the electrical stabilization of the MG, either for grid connected mode and for the islanded mode of operation.

If with synchronous generators, output control and power sharing is performed by the voltage regulator, governor and the inertia of the rotating machine in presence of renewable DERs, VSCs are used as interface for DC sources (like PV or batteries), or as part of back-to-back converters and require a specially designed control to simulate the inertia characteristic of synchronous generators and provide appropriate frequency regulation. Even the different configurations of variable speed wind turbines need power converter structures based on two AC-DC converters to extract the optimum power from the wind turbine while exchanging the appropriate reactive power with the power grid.

A general scheme with electronic interfaced sources in a MG is pictured below:

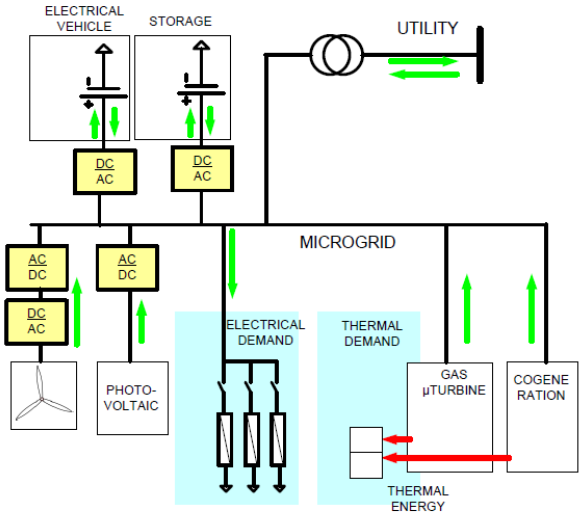

Fig. 2, Example of a typical microgrid scheme with generation and storage systems, from (Agust Egea-Alvarez, 2012)

For these purposes, power electronics controllers are composed of two stages: the DG power sharing controller and the converter output controller.

Power sharing controllers are responsible for the adequate share of active and reactive power mismatches in the MG whereas converter output controllers should control and regulate the output voltages and currents. Converter output control typically consists of an outer loop for voltage control and an inner loop for current regulation. Power sharing is performed without need for communication by using active power-frequency and reactive power-voltage droop controllers that emulate the droop characteristics of synchronous generators.

However, to achieve an optimal operation of the MG, a management control levels is required (secondary control) and with it a communication system to link it to the primary control, also referred to as field control level.

Secondary control, or MG Energy Management System (EMS), is responsible for the reliable, secure and economical operation of the MG in either grid-connected or stand-alone mode. This task becomes particularly challenging in isolated MGs with the presence of highly-variable energy sources where the update rate of the unit dispatch command should be high enough to follow the sudden changes of load and non-dispatchable generators (Daniel E. Olivares, 2014).

The aim of the EMS is to identify the optimal (or near optimal) Unit Commitment (UC) and dispatch of the available DER units, so that certain objectives are obtained. Permanent voltage and frequency deviations produced by the action of the primary control are also restored by the secondary control (Daniel E. Olivares, 2014).

Finally, tertiary control is the highest level of control and, depending on the necessities of the host power system, it sets long term and typically “optimal” set points.

This tertiary control is responsible for coordinating the operation of multiple MGs interacting with one another in the system, and communicating needs or requirements from the host grid (voltage support, frequency regulation, etc.) (Daniel E. Olivares, 2014).

This control level typically operates in the order of several of minutes, providing signals to secondary level controls at MGs and other subsystems that form the full grid. Secondary controls, on the other hand, coordinate internal primary controls within the MGs and subsystems in the span of a few minutes. Finally, primary controls are designed to operate independently and react in predefined ways instantaneously or within milliseconds to local events and to control the power flows and bus voltages (Daniel E. Olivares, 2014).

The converter constitutes the main element of interaction with the utility and an AC MG can include a single converter or multiple converters. The natural inclination of MGs tends to the decentralization of resources implying that more than one converter will be present in the system. This last option involves some implications on how a converter can be operated, mainly, regarding synchronization challenges.

Focus on this chapter will be put on the state of the art of primary control mode of operation, where real and reactive power generated within the MG, including the temporary power transfer from/to storage units, should be in balance with the shifting demand of local loads.

As said before, reliability issues are more significant and critical in stand-alone mode where the available power of the DG units must meet the total load demand of the MG or the system must undergo load shedding to make these match.

So that object of this chapter is focusing on grid-connected mode where the interaction with the main host grid is allowed to the possibility of being supplied possible power deficit or trading the excess power generated (providing ancillary services for example) with it.

Description of how the MG Central Controller (MGCC) system regulates the flow of active and reactive power through the operation of DER and the main grid, transition from/to the two modes of operation and the implementation of changes required in the control strategy with such mode transition will not be discussed in this thesis.

4.1 Primary Control

Primary control of electronically coupled DER units via power electronics in MGs has been discussed extensively in the technical literature.

There are different types of converters, for renewable generation and for other MG's elements integration into the grid. They can be classified depending on which kind of semiconductors they adopt and on their number of levels.

Voltage Sourced Converters (VSC) are based on Insulated-Gate Bipolar Transistors (IGBT) or similar technologies and they can provide fast switching and modulate any desired voltage. So that these devices are able to control independently active and reactive power, can supply black start capability and inject minimal harmonic distortion and currents allowing to use lighter filters (resulting compact in size). Main drawback is represented by the high losses provoked by the high frequency at which this power electronic appliance is operated (Agust Egea-Alvarez, 2012).

Line Commutated Converters (LCC) are instead based on thyristor or similar technologies that require the grid to be operated, as its turn-off and switching rely on the external circuit. LCCs are able to control active power while consuming non controllable reactive power, and as already said, they need the grid to be operated and require large filters for the important harmonic currents they generate. The main advantage is due to the fact that they allow for higher voltages and powers and they produce less losses commutating at much lower frequencies compare to VSC (at the grid frequency).

So that besides the above-mentioned features, for having switching independent of external circuits, possibility of changing current direction and to operate into weaker AC system, VSCs are commonly preferred for interfacing units into a MG environment.

Converters can be also classified depending on their number of levels. In LV applications (object of this work), it is common to use only two-levels and when voltages involved increase several semiconductors are placed in series. In this case, multilevel technologies can be used, using these multiple levels to modulate voltages with fewer harmonic content. There are several topologies of multilevel converters available and the difference lies in the mechanism of switching and the source of input voltage to the multilevel converters. These can be classified in multilevel configurations with diodes clamped, bidirectional switch interconnection, flying capacitors or cascaded H-bridge converters.

As using a two-level VSC converter (like it is done throughout this work) would produce unacceptable levels of harmonic distortion, some form of PWM is always used to improve the harmonic distortion of the converter. As a result of the PWM, the IGBTs are switched on and off many times (typically 20) in each mains cycle (hence the high losses and reduced overall transmission efficiency)-.

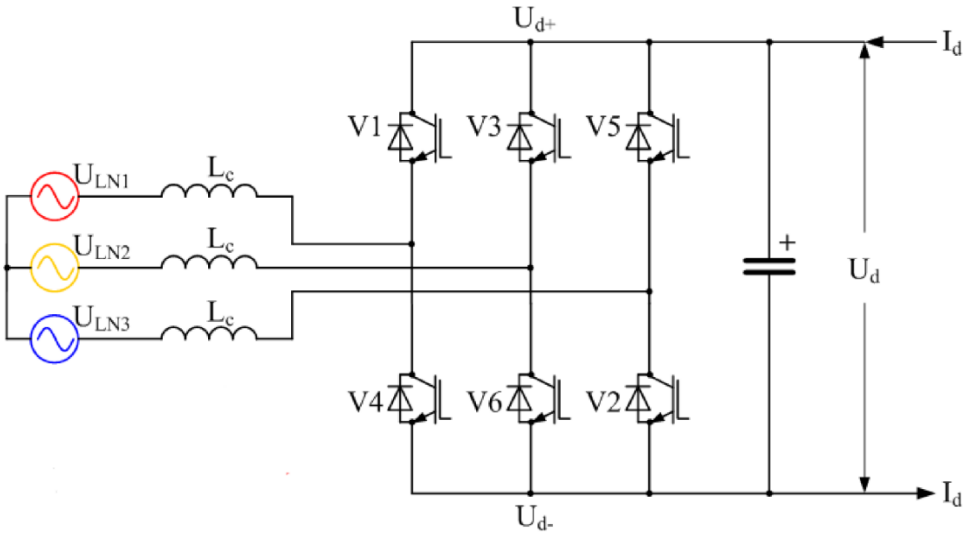

Fig. 3, Three-phase, two-level voltage-source converter using IGBTs, from (Wikipedia)

Although extensive research has been carried out on the development of MG primary control strategies, the following areas can benefit from further research (Daniel E. Olivares, 2014):

- improving robustness to topological and parametric uncertainties
- improving transient response of the controllers
- obviating the need for complex communication infrastructure

- developing control schemes that function for both grid-tied and islanded modes of operation of the MG and provide a smooth transition
- accounting for imbalance and harmonics
- enhancing scalability of the control schemes
- incorporating the DC-side dynamics in the control design
- improving fault ride-through capabilities

VSCs for being correctly operated as interface for DC sources, or as part of back-to-back converters, depend upon a specifically designed control to reproduce the inertia characteristic of a synchronous generators providing accordingly frequency regulation.

For this purpose, VSC controllers comprise of two stages: one addressed with a DG unit power sharing controller and one with the converter output controller.

Power sharing controllers are responsible for the adequate share of active and reactive power mismatches in the MG, whereas converter output controllers should control and regulate the output voltages and currents.

Converter output control usually consists of an outer loop for voltage control and an inner loop for current regulation. Power sharing is accomplished without requiring any communication by using active power-frequency and reactive power-voltage droop techniques that emulate the droop characteristics of synchronous generators.

4.1.1 Power sharing

A fundamental step included in the primary control is the power sharing control that can be classified based on whether or not it utilizes the concept of droop Converter output.

A power management strategy (PMS) is required for sound operation of a MG with multiple (more than two) DG units, particularly during the autonomous mode of operation. Since it is not part of the focus of the thesis for simplicity terms it will be just introduced and discussed in general terms.

Discussed in the next two paragraphs power sharing control techniques for MGs are discussed: droop methods and non-droop-based methods.

4.1.1.1 Droop methods

With a non-radial system configuration due to the presence of DG units, the power control complexity for a MG is substantially increased, and the “plug and play” feature is the key to ensure that the installation of additional DG units will not change the control strategies of DG units already in the MG. A popular approach to realize this “plug and play” characteristic is to employ the frequency and voltage droop control for real and reactive power regulation by mimicking the parallel operation characteristics of synchronous generators.

Droop methods for controlling DER units arises from the principle of power balance of synchronous generators in extensive interconnected power systems whereby the active power output of a single generator reduces as the line frequency increases and vice-versa. Equivalently its output reactive power variations originate from deviation in voltage magnitude of the grid.

The frequency power droop control method relates to the steady-state operation of conventional synchronous generators but can be artificially designed for electronically interfaced units too. In droop control, the relationship between real power/frequency and reactive power/voltage of a DG unit can be expressed as:

$$\omega_0 = \omega^* - K_p(P_0 - P^*)$$
$$V_0 = V^* - K_Q(Q_0 - Q^*) \qquad eq.1\ and\ 2$$

where the values ω^* and V^* correspond to the reference values for angular frequency and voltage, ω_0 and V_0 to the measured output frequency and voltage of the system (same for the active power P and reactive power Q) and K_v and K_p are the droop coefficients determined based on the steady-state performance criteria.

The main benefit of droop control is that it removes the need for communication (the control action is simply based on local measurements) resulting in significant flexibility where, as long as the balance between generation and demand is maintained, there is no interdependency between the local controllers, i.e., the controller carries out tasks based on local measurements and droop characteristics suitably.

Main drawbacks of droop control include:

- instability issues due to the use of average values of active and reactive power over a cycle
- Overlook of load dynamics that can cause a failure after a large or fast load change.
- incompatibility for black-start-up after system breakdown
- Poor performance when adopted for LV distribution networks where, due to a low X/R ratio, coupling between active and reactive power is strong
- Unsuitability for nonlinear loads since it does not consider harmonic currents
- Inability to establish a fixed system frequency independent of the load evolution of the system

Different alternatives have been investigated in literature to address power sharing within a MG.

In (Yasser Abdel-Rady Ibrahim Mohamed, 2008) with an eigenvalue analysis of a linearized microgrid system it can be seen that the conventional droop controller lacks the ability of controlling the damping of the low-frequency power modes at different operating conditions without affecting the frequency regulation, which is a stiff requirement at steady-state operation. The damping factors of the aforementioned slower modes migrate to lower values when the active power output of the DG unit is increased, relative stability is remarkably affected and power oscillations are yielded.

To overcome the aforementioned difficulties, a designed power sharing controller adopts a modified droop function with controllable gain transient droop characteristics. This configuration leads to a 2-DOF tunable controller, where the droop gain is selected to determine the frequency/voltage regulation performance and adaptive transient droop gains are tuned to damp the oscillatory modes at different operating conditions. The proposed controller achieves a robust power sharing performance with simple PI structure and easily derived adaptation gains.

In (Units F. Katiraei, 2009) the active power management an electronically interfaced DG unit is specified based on a frequency-droop characteristic and a frequency restoration algorithm is introduced. This method is chosen since the frequency of the MG, during an autonomous mode of operation freely varies when none of the DG units can dominantly enforce the base frequency of the system.

In a LV MG, the operation is further complicated when considering the large variation of electrical distance between DG units even within a small geographical area. This variation of electrical distance is caused by different DG interfacing topologies. E.g., for direct coupled DG units, the impedance between two DGs could be just the LV distribution feeder, which has very small inductance and high ratio, while in the case of DG units with grid coupling inductors and/or with transformers, the equivalent electric distance among DGs is comparable to medium and long transmission lines.

For reactive power control, (Kao, 2009) proposes a virtual inductor at the interfacing converter output and an accurate power control and sharing algorithm with consideration of both impedance voltage drop effect and DG local load effect. In grid-connected mode to avoid $P-Q$ coupling, virtual real and reactive powers can be used (K. D. Brabandere, 2007), which are decoupled through frame transformations with the line impedance angle information. While effective for power control in grid-connected mode, this method cannot directly share the actual real and reactive powers between the DG units in MG islanding operation mode. In order to control the decoupled real and reactive power flows in a similar manner as the conventional power system with a high X/R ratio, a method employed in this paper is to control the DG interfacing converter with a virtual output inductor that introduces a predominantly inductive impedance without the need of line impedance information. Specifically, the virtual inductance can effectively prevent the coupling between the real and reactive powers by introducing a predominantly inductive impedance even in a LV network with resistive line impedances (where a ''normal'' droop method is subject to poor transient and poor stability due to the real and reactive power coupling among DG units) when no additional inductance is present. On the other hand, based on the predominantly inductive impedance, the proposed accurate reactive power sharing algorithm functions by estimating the impedance voltage drops and significantly improves the reactive power control and sharing accuracy.

In (Li, 2011) the proposed real and reactive power control is based on the virtual frequency and voltage frame, which can effectively decouple the real and reactive power flows and improve the system transient and stability performance.

4.1.1.2 Non-Droop-Based Methods

These class of methods address power control and management in a more centralized perspective.

In (C. K. Sao and P. W. Lehn, 2008) a centralized controller is proposed as part of a solution where the total load current is measured and transmitted to this. After this, the contribution of each unit is computed and output current reference set points are dispatched back to the units, depending on the features of each of these while an outer loop simultaneously controls the voltage of the system. This method proves to be fast in mitigating the transients but a well-thought communication scheme results crucial with a possible failure of this leading to failure of the whole system.

A method for voltage control and power sharing among multiple parallel DER units in close electrical proximity in a MG is proposed in (Green, 2006). This means that the generators are connected to a common bus before connection to the distribution network or MG. This method utilizes a communication link of

limited bandwidth to achieve power sharing between the different units and voltage control through a central controller. Local controllers are responsible for harmonic and imbalance rejection. Steady-state and low-frequency (principally unbalanced) issues are controlled centrally and, as said, a low-bandwidth communication channel is employed to distribute control signals to individual units. For addressing high-frequency issues like harmonic suppression, each converter operates locally without the use of a communication channel that so it is used where it can have most effect and where the bandwidth requirement will not be onerous or expensive to implement (Green, 2006). The intention is to achieve approximately the same control performance from a set of parallel units as could be obtained from a single unit of the combined rating.

Another example of effective power sharing management without involving droop techniques is depicted in (Bilal Mouneir, 2014), even though it specifically addresses operation of the MG in stand-alone mode.

A master-slave control strategy, where a dominant DG unit and its VSI, acting as a master, guarantee to keep the system voltage within a permissible range and it is used as voltage reference as other units supply the load operating in P-Q mode (slaves). As can be noted such functioning mechanism it is based on the conventional power system operation in which a slack bus controls frequency and voltage, and a number of PQ-buses either inject or absorb active and reactive power. As long as the balance between the load and generation is maintained, this method is flexible with respect to connection and disconnection of DER units although presence of a dominant DG unit is crucial.

4.1.2 Output control

A number of control schemes have been suggested in literature to approach the control of power converters with feed-back controlled converters showing numerous and relevant advantages compared to open loop-controlled ones. Namely adaptability and robustness to disturbances on the grid and to different operation points, fast response and higher stability have proven necessary in most applications and have made feedback control almost unavoidable.

The converter output control typically consists of an outer loop for voltage control, and an inner loop for current regulation.

A general overview of grid-side converter controllers is given in (F. Blaabjerg, 2006), in which controllers are classified based on their reference frame: synchronous ($\alpha\beta$), stationary (qd), and natural (abc). The synchronous reference frame is associated with DC variables and Proportional-Integral (PI)-based controllers while the stationary reference frame with sinusoidal variables and Proportional- Resonant (PR) controllers. The natural reference frame employs controllers realized in the form of PI, PR, hysteresis, or dead-beat.

The feedback control techniques for power converters can be roughly classified between linear control theory-based designs and nonlinear controller designs.

4.1.2.1 Linear

The linear theory designs are based on the averaged model of the converter, which considers the control action to be able to change continuously despite the discrete number of possible switching states of the converter. This allows to apply the well-known and established linear control theory techniques to model and evaluate the system, providing plenty of information on how this will behave under different scenarios.

At the same time, it is necessary to use PWM technique, such as the sinusoidal PWM and the space vector PWM, for converting the voltage output reference from the current controller into the switching signals sent to the actual converter switching devices.

For calculation of the controller output, normally a variable transformation matrix is applied to the measured values of the variables. Utilizing the so known Park reference transformation matrix using a reference angle that corresponds to the grid angle (the so called synchronous reference frame), both voltage and current magnitudes become constant in steady state under grid balance conditions, making it possible to use classical PI regulators on the control loops hence simplifying a lot the design of the controllers (Agust Egea-Alvarez, 2012).

But as this benefit is lost under unbalanced conditions, some authors propose either to employ an enhanced double synchronous reference frame (Nam, 2011) where with imbalanced voltages would have deteriorated the performance of a PWM converter introducing by producing higher voltages voltage ripples in the DC link. So that using two synchronous reference frames, rotating in opposite directions, since the positive and the negative sequences appear DC in their own frames, each can be measured separately by using an higher frequency notch filter (to eliminate the higher frequencies components in each frames) and used for two feedback PI controllers, namely the dual current controller.

Another possible solution is the utilization of the Clarke transformation instead (the so called stationary reference frame) which requires PR regulators but enables proper operation of the system under such condition (He, Modeling and control of grid-connected voltage-sourced converters under generalized unbalanced operation conditions, 2008).

If in (Nam, Dual Current Control Scheme for PWM Converter Under Unbalanced Input Voltage Conditions, 2009) it is necessary the use of sub-sequential component decomposing filters that might narrow the controller bandwidth and overall stability margin, in the proposed solution a new current regulator based on the PR scheme is implemented. This directly regulates the overall current including both positive and negative-sequence components in the stationary $\alpha\beta$ frame. Unlike the traditionally dual current regulators like in (Nam, Dual Current Control Scheme for PWM Converter Under Unbalanced Input Voltage Conditions, 2009), in which there exist DC signals in the positive and negative synchronously rotating reference frames, these proposed current regulators, have AC values with multifrequency components. The simulated and experimental results demonstrate the control scheme to provide sufficiently steady-state tracking capability for AC input current and a better transient response in compensation for wide-range generalized unbalanced operation conditions.

4.1.2.2 Non-Linear

Although the PI controller assures zero steady-state error for continuous reference, it can present such an error for sinusoidal references. This error increases with the frequency of the reference current and may become unacceptable for certain applications.

On the other hand, nonlinear based designs usually consider the discrete nature of the converter state and that only a finite number of possible switching states can be generated by this and that models of the system can be used to predict the behavior of the variables for each switching state.

The controllers output the switching commands for the converter devices instead of using PWM. This makes it possible to obtain a faster response and is said to be less dependent on the system parameters but makes the system harder to study due to the higher complexity and the lower availability of the analysis tools for nonlinear systems. Among the nonlinear techniques the most well-known are those based on the so-called Direct Power Control (DPC).

In (Toshihiko Noguchi, 1998) it is proposed a control technique of the PWM converter, which makes it possible to achieve an improved power factor by directly controlling its instantaneous active and reactive power without any voltage sensors. The controller features relay control of the active and reactive power by using hysteresis comparators and a switching table. By using this switching table, the optimum switching state of the converter can be selected uniquely in every specific moment according to the combination of the digitized input signals. The selection of the optimum switching state is performed so that the power errors can be restricted within the hysteresis band (load currents are forced to remain within the hysteresis band).

Second key point is an estimation technique of the voltages for sensor-less operation based on an evaluation of the instantaneous active and reactive power for every switching state of the converter, which can be used as the feedback signals to the power controller.

Main drawbacks of this method are the non-constant switching frequency, which can cause resonance problems, makes more difficult the computation of losses of the power electronic device and to correctly design the switching noise filters.

To avoid this, other techniques such as current predictive control can be implemented. Current control is one of the most important and classical subjects in power electronics and has been extensively studied in the last decades and as well documented as nonlinear methods, like hysteresis control and linear methods previously briefly discussed in this chapter.

In (José Rodríguez, 2007) for the selection of the appropriate switching state of the converter to be applied, a selection criteria is defined and expressed as a quality function that is then evaluated for the predicted values of the variables to be controlled. Prediction of the future value of these variables is calculated for each possible switching state and the switching state that minimizes the quality function is finally selected.

To conclude the chapter it is important to remark that the most common and widely adopted approach for designing the control loops of a VSC is by using linear methods and PI controllers with additional feed-forward compensation to increase and better the performance of current regulators. So that a control scheme able to control independently active and reactive power based on the instantaneous power theory in the synchronous reference for DG and storage systems connected to the grid by means of VSCs is fully described and justified in Chapter 5.

After an introduction on the theory, each and every necessary block of a VSC average model (including the phase locked loop, the current references calculation, the currents controllers and DC bus voltage controllers) is described and detailed. Simulation results are eventually included to illustrate the dynamic performance of the control scheme and exemplify the described control approach.

5. Description of the electrical system and VSC average model

As previously widely stated, power electronics and more specifically VSCs are the enabling technologies to convert classical power systems into smart grids, since they allow controlling the power flows and bus voltages within milliseconds range.

For their ability to optimize energy extraction from RS while exchanging bidirectionally power with the grid they became in the last decades key elements in MGs and DG systems (Agust Egea-Alvarez, 2012).

For instance, to decouple the dynamics of a wind power generator from the grid, whose generation is of variable AC frequency, a rectifier transforms output of this generator to DC before injecting the power to the main power system as part of a back-to-back converter arrangement. At the same time, as the load for batteries and PV power systems is of DC nature, in most applications this is transformed and regulated using DC/DC converters before being converted by DC/AC converters for interfacing the grid.

The average model of a VSC discussed and modelled in this chapter has been developed mainly following the paper (Agust Egea-Alvarez, 2012).

The system object of analysis is represented schematically in Fig. 4, where the considered grid is of a three-phase three-wire kind and the two-level VSC exchanges power between the AC side and the DC side.

The converter is composed of three branches with two Isolated Gate Bipolar Transistors (IGBTs) each. The middle point of each branch is smoothly connected to one different phase of the grid by means of inductances to allow for a smooth connection to the grid of the device. Antiparallel diodes are connected to the IGBTs in order to avoid extremely high peaks of voltage across the transistors produced by the inductances when these react to high current derivatives.

Appropriate modulation or commutation cycle of the IGBT switching allow to generate the desired three-phase voltages on the AC side to control the active and reactive power flow.

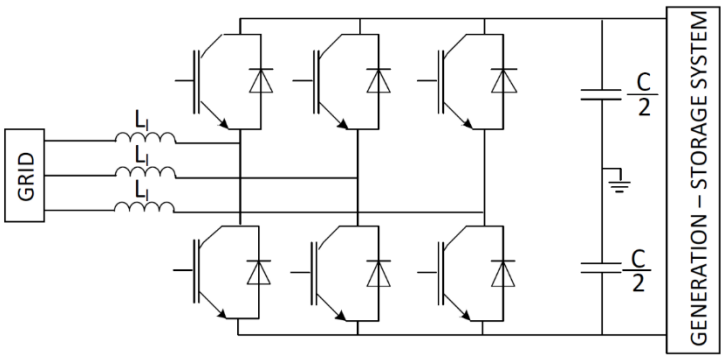

Fig. 4, System under analysis comprising the VSC converter and the three-phase utility grid, from (Agust Egea-Alvarez, 2012)

The power generation or storage source is connected to the DC side that can be modelled as a current source connected to a shunt capacitor (as done for simulation involving renewable power generation, first discussed in this chapter) or as a DC voltage source (used for simulation with storage power generation) while the AC side is modelled as the utility grid Thevenin equivalent.

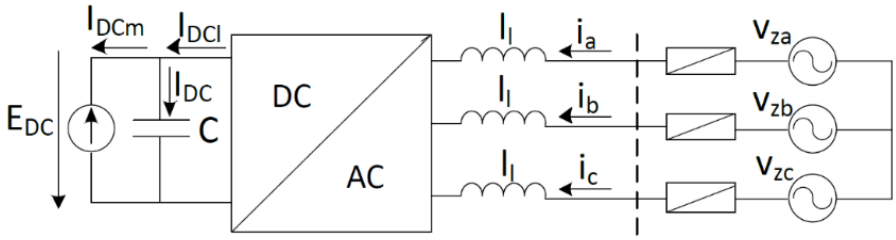

Fig. 5, VSC with the DC side modelled as a current, from (Agust Egea-Alvarez, 2012)

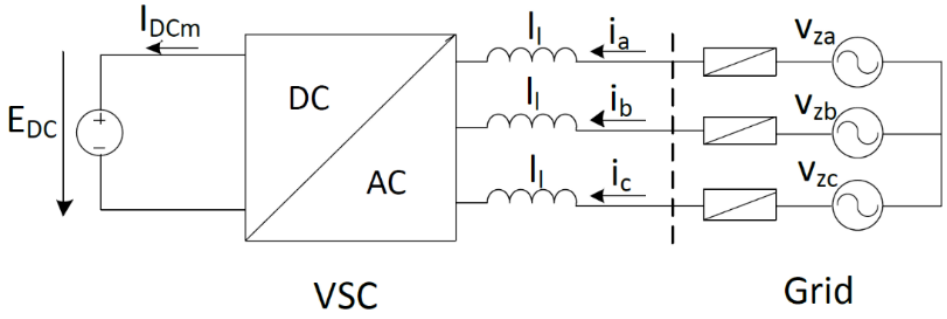

Fig. 6, VSC with the DC side modelled as a voltage source, from (Agust Egea-Alvarez, 2012)

Again, for simplicity, although the VSC is based on the discrete states of the switching of the IGBTs, for control design purposes it is convenient to derive a more simplified equivalent model.

Using MATLAB/Simulink software an average model of the converter has been built so that the transistors have not been modelled and only average powers have been considered for the operation.

Doing so, the commutation losses in the IGBTs are neglected and the PWM control for the transistors is unnecessary and will not be further discussed throughout this work.

The aim of such simplified modeling is less complexity and faster time domain simulation studies of the grid connected converter. The model eventually proved to be efficient and fast for the computation maintaining sufficient converter dynamic accuracy.

5.1 VSC model

The VSC permits to control two electrical variables in a synchronous frame so that separate control of the active and reactive power is allowed. The reactive power reference is acquired from a higher control level (grid operator or simply the user) or set to a given value while the active power reference depends on the nature of the source connected in the DC side:

- For renewable energy systems, it is adjusted to regulate the DC bus voltage and to ensure the power balance meaning that power injected into the grid has to be the same as the generated power

- For storage systems, it is adjusted to charge the battery or to inject power to the grid depending on the operation of the EMS of the MG or system where the storage system is connected

Renewable energy generation is first considered, since it is a more complex case where a DC voltage controller is needed. For storage systems it is enough to remove the DC voltage controller and establish the active power reference straightforward.

The model has been developed using MATLAB/Simulink software package and it is built up by few blocks that can be divided into two main subsystems:

- The power subsystem that is directly connected to the DC generation component and to the AC grid. This receive inputs from the control subsystem to correctly interface the DC source, whose voltage is controlled and maintained stable, with the grid.

- The control subsystem (composed in turn by few sub-blocks) at which reference signals from a higher level control system are sent and inputs from the grid are taken. Once this calculates the correct values for the proper functioning of the whole power system, these signals are sent to the converter to be performed.

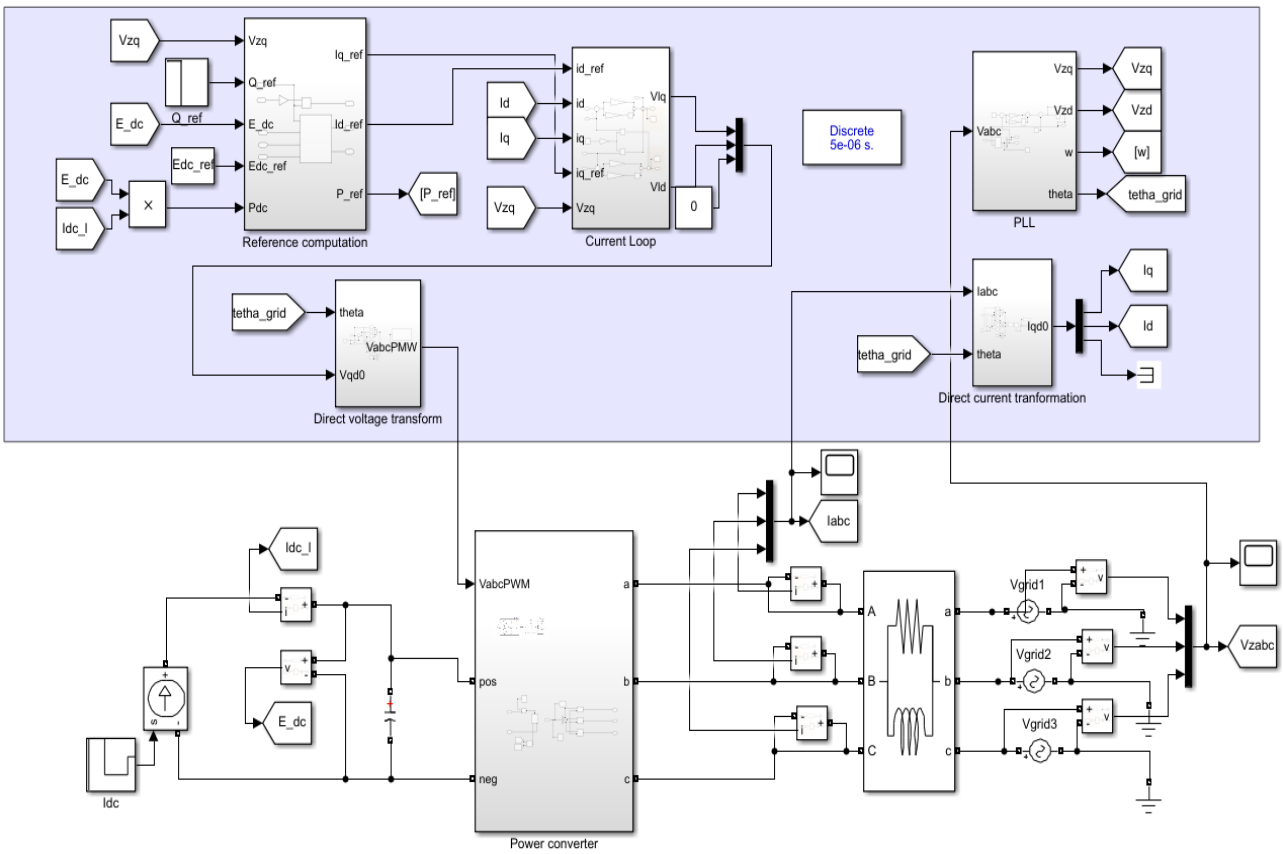

Fig. 7, Average model for the VSC converter, created with MATLAB/Simulink. To the left the DC source modelled as a programmable current source, in the center the power subsystem, to the right the AC three-phases grid modelled as three controlled voltage sources

5.1.1 Power subsystem

A simplified model can be derived decoupling the DC and AC parts of the converter as illustrated below:

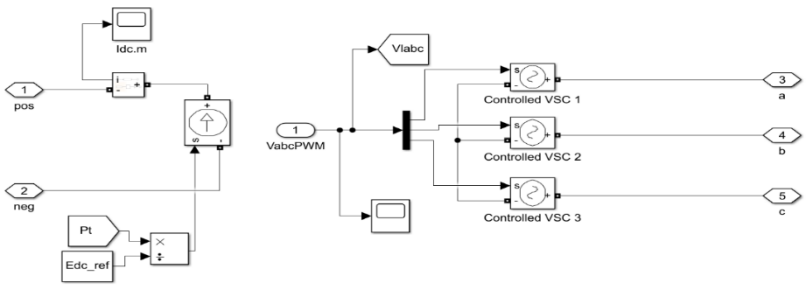

Fig. 8, Average model for the power subsystem block created with MATLAB/Simulink

The AC side is modelled with three AC controlled voltage sources (one for each phase of the grid) since they operate at variable voltages depending on the control action input and executed.

The current source in the DC side reflects the active power exchanged between the AC and the DC side and assures the system power balance and it can be computed neglecting converter losses as:

$$I_{dc} = \frac{P_t}{E_{dc,ref}} \qquad eq.3$$

5.1.2 Control subsystem

The control scheme relies on a two-level cascaded control system, where the lower level controller deals with regulation of the AC current in the qd components, while the higher-level controller deals with the necessary regulation the DC bus voltage.

As shown later, a phase Locked Loop (PLL) to track the grid angle is needed as both level controllers deal with currents and voltages in the $qd0$ synchronous reference frame rotating to adjust the electrical grid angle.

A graphical explanation of the general control scheme is depicted below. As briefly mentioned before, as a simplified model of the VSC is treated in this work, the voltage modulation block has not been modelled or used as the PWM control for the transistors is out of scope for this project.

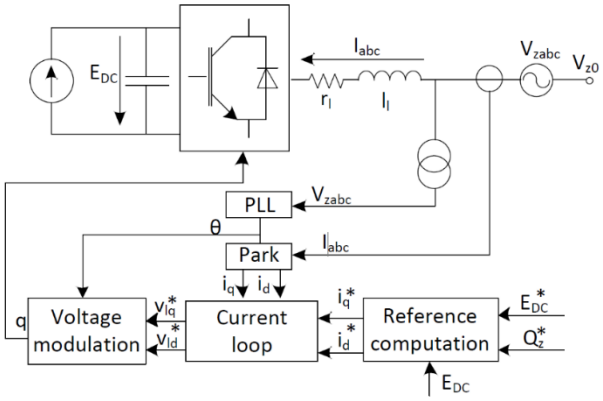

Fig. 9, Grid converter control general scheme for renewable energy generation systems, from (Agust Egea-Alvarez, 2012)

The control scheme comprises a few blocks and can be schematically described within five subsequent steps:

1. First the three phase voltages currents and voltages $Iabc$ and $Vabc$ are tranformed through a Park tranformation into $Iqd0$ and $Vqd0$.

2. these voltages go into a phase locked loop that not only computes the electrical grid angle but also ensures that $Vd = 0$.

3. The current references $Idref$ and $Iqref$ to obtain the desired active and reactive powers $Qref$ and $Pref$ are obtained from the instantaneous power theory in the reference computation block (that contains within itself the DC voltage regulator block)

4. In the current loop control block the reference converter side voltages $Vlqref$ and $Vldref$ are computed from the input transformed measured grid currents and the reference currents from the previous block.

5. These voltages are sent to the final block 'direct voltage transform' that implement an inverse park transformation to transform $Vlqref$ and $Vldref$ into the actual voltages $Vlabc$ to be executed by the AC side of the power converter.

Direct and inverse Park transformation

The quantities in the stationary frame $\alpha\beta$ discussed in (Agust Egea-Alvarez, 2012) are useful in a number of applications but have the same oscillating nature as the quantities in the abc frame. For the controller design it is useful to have constant quantities. And this can be achieved by implementing the Park transformation (Nee., 1998) and the so-called synchronous reference frame. The Park transformation is a tensor that rotates the reference frame of a three-by-three element matrix in an effort to simplify the analysis (Wikipedia, Direct-quadrature-zero transformation), hence in this case the control loops that will follow in the control scheme described before, allowing the use of simple PI controllers.

After a time-ramp transient, the corresponding transformed value are equivalent to the peak values of a generic harmonic function. Below an example of three phase balanced voltages after such transformation.

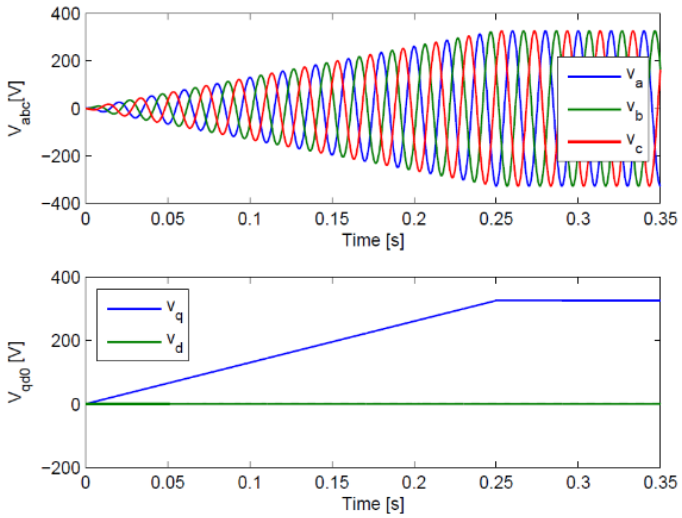

Fig. 10, Example of three-phase voltages in the abc and qd0 frames, note how vd is kept to a constant null value, from (Agust Egea-Alvarez, 2012)

This transformation extremely simplifies the control of three-phase voltages and currents and can be expressed by the equations

$$[x_{qd0}] = [T_{qd0}][x_{abc}] \quad eq.4$$

and its inverse,

$$[x_{abc}] = [\,T_{qd0}]^{-1}[x_{qd0}] \quad eq.5$$

where $xabc$ is a vector with the three phase quantities in the abc frame and $xqd0$ is a vector with the transformed quantities in the $qd0$ frame. The transformation matrix T can be written as

$$T\,(\theta) = \frac{2}{3}\begin{bmatrix} cos\,(\theta) & cos\left(\theta - \frac{2\pi}{3}\right) & cos\left(\theta + \frac{2\pi}{3}\right) \\ sin\,(\theta) & sin\left(\theta - \frac{2\pi}{3}\right) & sin\left(\theta + \frac{2\pi}{3}\right) \\ \frac{1}{2} & \frac{1}{2} & \frac{1}{2} \end{bmatrix} \quad eq.6$$

And its inverse

$$T^{-1}(\theta) = \begin{bmatrix} cos\,(\theta) & sin\,(\theta) & 1 \\ cos\left(\theta - \frac{2\pi}{3}\right) & sin\left(\theta - \frac{2\pi}{3}\right) & 1 \\ cos\left(\theta + \frac{2\pi}{3}\right) & sin\left(\theta + \frac{2\pi}{3}\right) & 1 \end{bmatrix} \quad eq.7$$

Where the parameter theta is the instantaneous electrical angle of the first phase a, which is calculated in the Phase Locked Loop (PLL) block. The Park transformation can be also visually seen as a geometric transformation combining the Clarke transformation with a rotation as illustrated below.

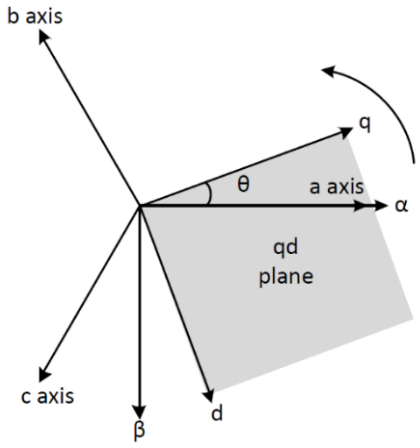

Fig. 11, qd plane representation, from (Agust Egea-Alvarez, 2012)

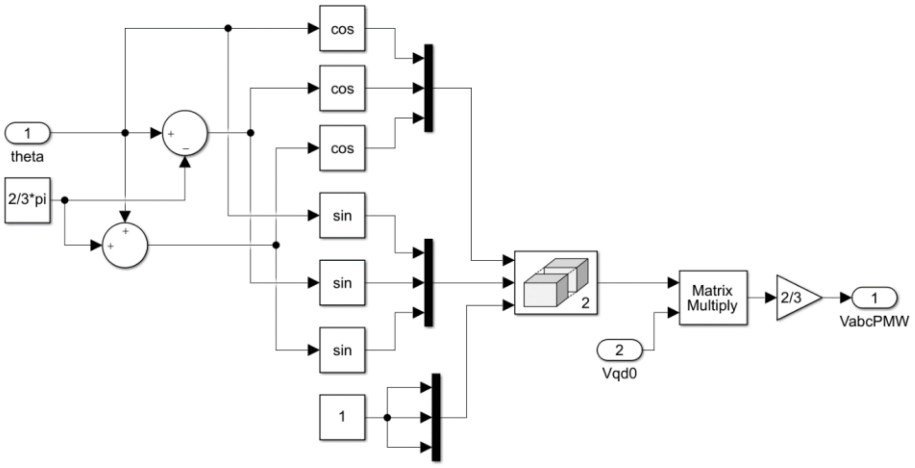

Fig. 12, Inverse Park transformation block for the voltages created with MATLAB/Simulink following equations 5 and 7

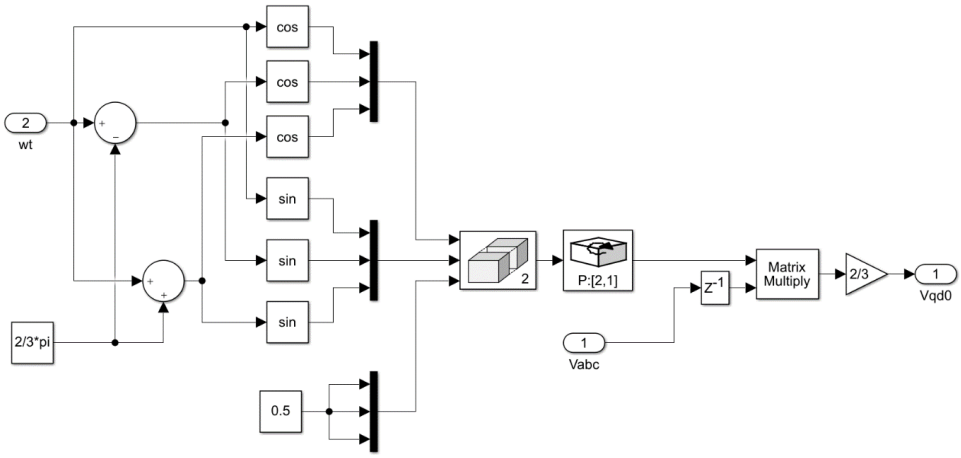

Fig. 13, Direct Park transformation block for the voltages created with MATLAB/Simulink, following eq. 4 and 6

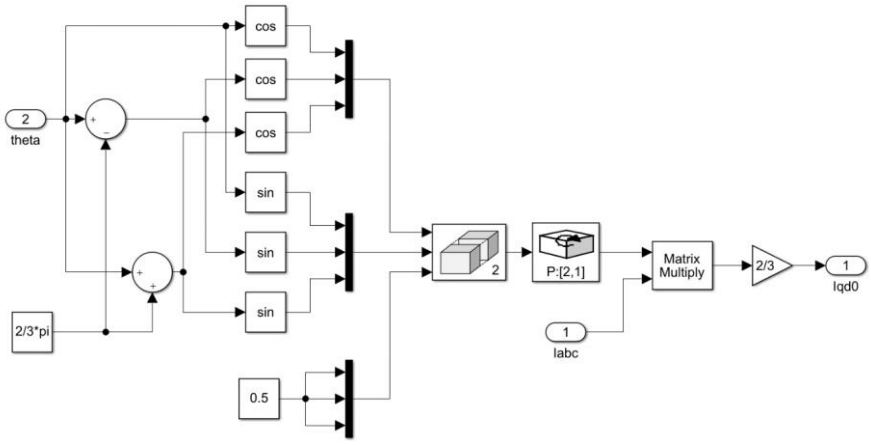

Fig. 14, Direct Park transformation block for the currents created with MATLAB/Simulink, following eq. 4 and 6

Phase locked loop

A PLL is implemented for the computation of the angle and the angular speed of the electrical network. A three-phase PLL consists in a feedback of the $d-axis$ filtered by a PI controller with a 0 reference, so that other purpose of the PLL is to stabilize the voltage Vzd to a costant null value.

The output of the controller corresponds to the angular velocity ω of the electrical grid and the integration of this signal corresponds the grid angle θ. A usual scheme for a PLL is depicted below.

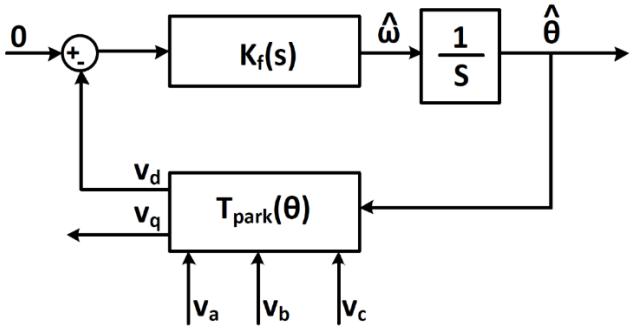

Fig. 15, , Schematic of a PLL, from (Agust Egea-Alvarez, 2012)

It can be seen that the PLL functions as a typical closed-loop feedback system to be solved iteratively as, for implementing the direct voltages Park transformation the grid angle θ, it is needed but, at the same time, for computing this angle the Park transformation block is necessary.

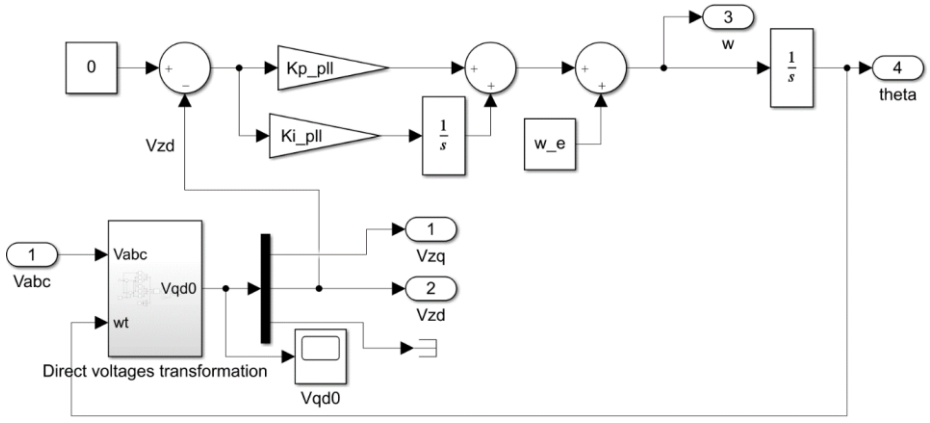

Fig. 16, implemented PLL system created with MATLAB/Simulink (with Park transformation block in it giving feedback to the PI controller) , following eq. 8, 9 and 10

Block has been built according to these formulas:

$$K_f(s) = \left(K_{p,PLL} + \frac{K_{i,PLL}}{s}\right) + we \qquad eq.\ 8$$

$$K_{i,PLL} = \frac{1}{\tau_{PLL}} \qquad eq.9$$

$$we = 2\pi f_e \qquad eq.10$$

Kp is the proportional gain and Ki the integrator gain for the PI controller, we is the angular velocity, τ_{PLL} is the time constant of the PLL and f is the frequency of the three-phases grid voltages.

Values of $20ms$ for the time costant and $Kp = 1$ has been considered for correct functioning of the PLL. After the Park transformation three-phase voltages $Vabc$ will look like Fig.10 already shown in this chapter.

Reference computation

The current references id and iq to obtain the desired active and reactive powers P and Q can be obtained from the instantaneous power theory. The Phase Locked Loop system as already said ensures that $vd = 0$. Substituting it in the equations below (from instantaneous power theory, (Agust Egea-Alvarez, 2012)), active power and reactive power P and Q are expressed as follows:

$$P = \frac{3}{2}\left(V_q i_q + V_d i_d\right) = \frac{3}{2} V_q i_q \qquad eq.11$$

$$Q = \frac{3}{2}\left(V_q i_d + V_d i_q\right) = \frac{3}{2} V_q i_d \qquad eq.12$$

So that:

$$i_q^* = \frac{2P^*}{3V_{z,q}} \qquad eq.13$$

$$i_d^* = \frac{2Q^*}{3V_{z,q}} \qquad eq.14$$

But since only direct reference for the first study case (with renewable energy generation) has been given for the reactive power $Qref$ (from the user) only $idref$ is directly computed in this block.

$Iqref$ is instead provided by the output of the voltage controller implemented to control the voltage of the DC bus ensuring power balance between the generation source and the power injected to the grid.

The proposed control scheme is depicted below, where the controlled quantity is E^2 and a feed-forward scheme is used to improve the system response. This is a common practice, since E^2 is proportional to the energy stored in the capacitor, and the output of the controller is the active power injected to the capacitor Pc. Therefore, the power reference for the power converter will be $P = Pc + Pdc$, where Pdc is the measured power before the capacitor.

As said $Pref$ is computed with a feedback PI controller.

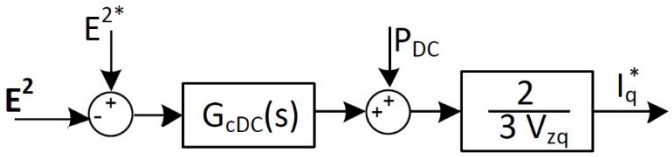

Fig. 17, Voltage controller scheme, from (Agust Egea-Alvarez, 2012)

Other formulas to model the block:

$$P^* = P_c^* + P_{dc} \qquad eq.15$$

$$P_{dc} = E_{dc} I_{dcm} \qquad eq.16$$

$$P_c^* = G_{cdc}(s)\left(E_{dc}^{*2} - E_{dc}^2(s)\right) \qquad eq.17$$

$$G_{cdc}(s) = K_{p,dc} + \frac{K_{i,dc}}{s} \qquad eq.18$$

$$K_{p,dc} = C\varepsilon_{dc}\omega_{dc} \qquad eq.19$$

$$K_{i,dc} = \frac{C\omega_{dc}^2}{2} \qquad eq.20$$

Other parameters to be take into account are: $Idcm$ the current in the DC bus (before the capacitor), C the capacitance of the capacitor equal to $1020\mu F$, ε_{dc} and ω_{dc} that are, respectively, the dumping ratio and the angular velocity that describe the second-order dynamics of the DC voltage and that can be modified in order to have different dynamics for the loop like a faster transient or smaller overshoot. Values chosen are $\varepsilon = 0.707$ and $\omega_{dc} = 418.88 rad/s$.

Worth mentioning that as it can observe, the DC voltage loop must be much slower than the inner current controller in order to assure a stable system response.

Below the blocks modelled using MATLAB/Simulink.

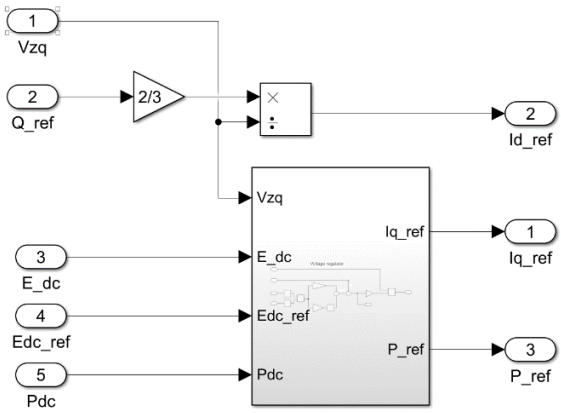

Fig. 18, Reference current computation block, created with MATLAB/Simulink

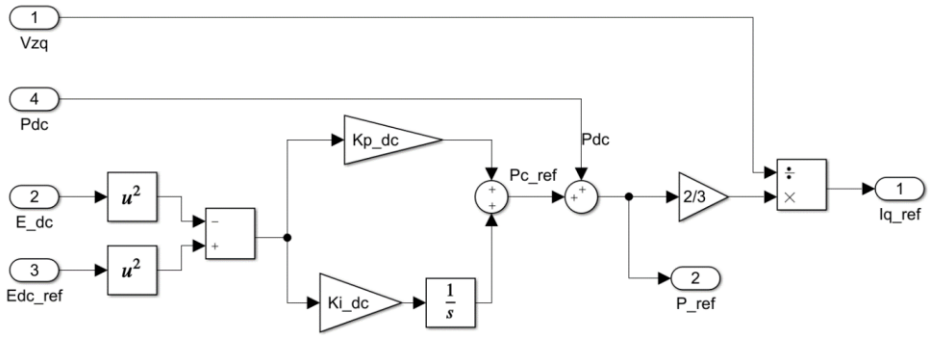

Fig. 19, Voltage Regulator with second order dynamics imposed to the DC voltage and reference for the active power is computed, created with MATLAB/Simulink

Current loop

With the current loop final voltages in the $qd0$ frame $Vzqref$ and $Vldref$ are computed for being later output to the final block where an inverse Park transformation is performed and these are converted into the actual voltages $Vlabc$ to be executed by the AC side of the power converter. Voltage equations are expressed by

$$\begin{bmatrix} v_{zq} \\ 0 \end{bmatrix} - \begin{bmatrix} v_{lq} \\ v_{ld} \end{bmatrix} = \begin{bmatrix} r_l & l_l\omega_e \\ -l_l\omega_e & r_l \end{bmatrix} \begin{bmatrix} i_q \\ i_d \end{bmatrix} + \begin{bmatrix} l_l & 0 \\ 0 & l_l \end{bmatrix} \frac{d}{dt} \begin{bmatrix} i_q \\ i_d \end{bmatrix} \qquad eq.21$$

Where r_l and and l_l are, respectively, the inductance equivalent resistance, and the inductance value (respective values of $0.5\ \Omega$ and $5.4\ mH$) and ωe the electrical angular velocity previously computed by the PLL.

It can be noted coupling between q and d currents and voltages in the equation above so that to control indipendently the input currents Iq and Id, a decoupling control approach is implemented using the Internal Model Control technique (Nee., Model-based current control of ac machines using the internal model control method, 1998) (rather than Multi-variable control, controlling the qd components with a single two dimension controller, as discussed in (Iravani, 2008), resulting overall too complex for the object of this work).

Below a graphical scheme of the system:

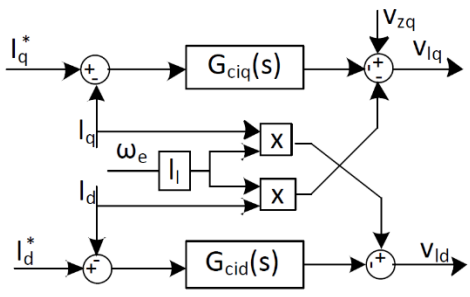

Fig. 20, Current controller scheme, from (Agust Egea-Alvarez, 2012)

Where

$$G_{ciq}(s) = G_{cid}(s) = \frac{K_p s + K_i}{s} \qquad eq.22$$

And the constants can be calculated as

$$K_p = \frac{l_l}{\tau} \qquad eq.23$$

$$K_i = \frac{r_l}{\tau} \qquad eq.24$$

where τ is the closed loop time constant of the system with a value chosen taking into account the converter physical restrictions and normally a number of times faster than the converter switching frequency (feature out of scope in this project). In this case $\tau = 1\ ms$.

Below the Current Loop block modelled using MATLAB/Simulink.

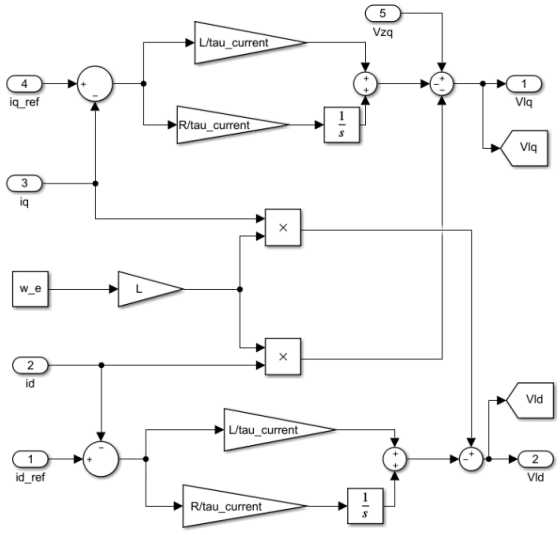

Fig. 21, Current Control block (with a first-order dynamics control qd currents to their references) created using MATLAB/Simulink, following eq. 22,23 and 24

5.2 Simulation results

5.2.1 Renewable energy generation

In this first simulation, the DG system injects the power to the electrical grid, therefore the VSC has to control the DC voltage in order to guarantee power balance i.e. the power injected into the grid has to be the same as the generated power.

A general scheme of the system is depicted in Fig.9.

As already specified in the paragraph regarding the modelling of each single block composing the system, the time constant of the current loop is set to $1\ ms$, while the natural frequency of the DC voltage regulator is equal $418{,}88\ rad/s$ (15 times slower than the current loops, as recommended in cascaded controllers) and finally $\varepsilon = 0.707$.

The presented simulation assesses the controllers' behavior for variations of the generated power. The generation power changed by changing the current of the DC source and the reactive power setpoints are as input with the following Simulink table:

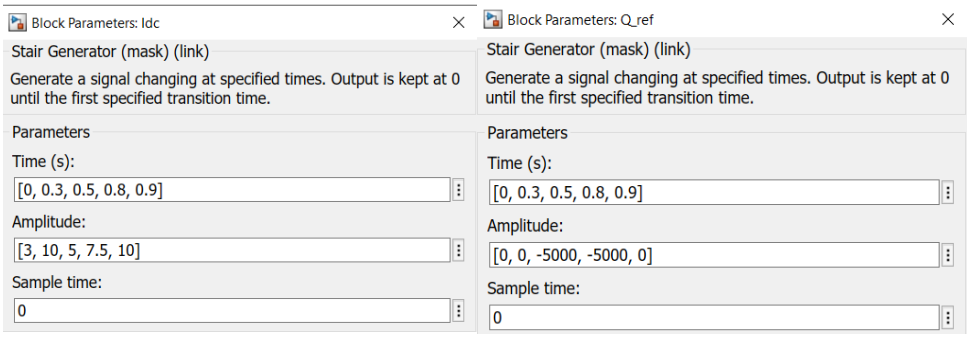

Fig. 22, Input parameters for Idc and Qref

Currents

Fig.23 shows the evolution of the qd VSC actual currents and reference currents current in the qd and abc reference frames. Current iq changes each time that DC current changes according to Table1 while id changes according to the reactive power reference. Id current, as can be deduced looking at the picture, clearly shows a first-order graph dynamic (being computed directly by $Qref$ and a PI controller) while Iq follows a second-order dynamic.

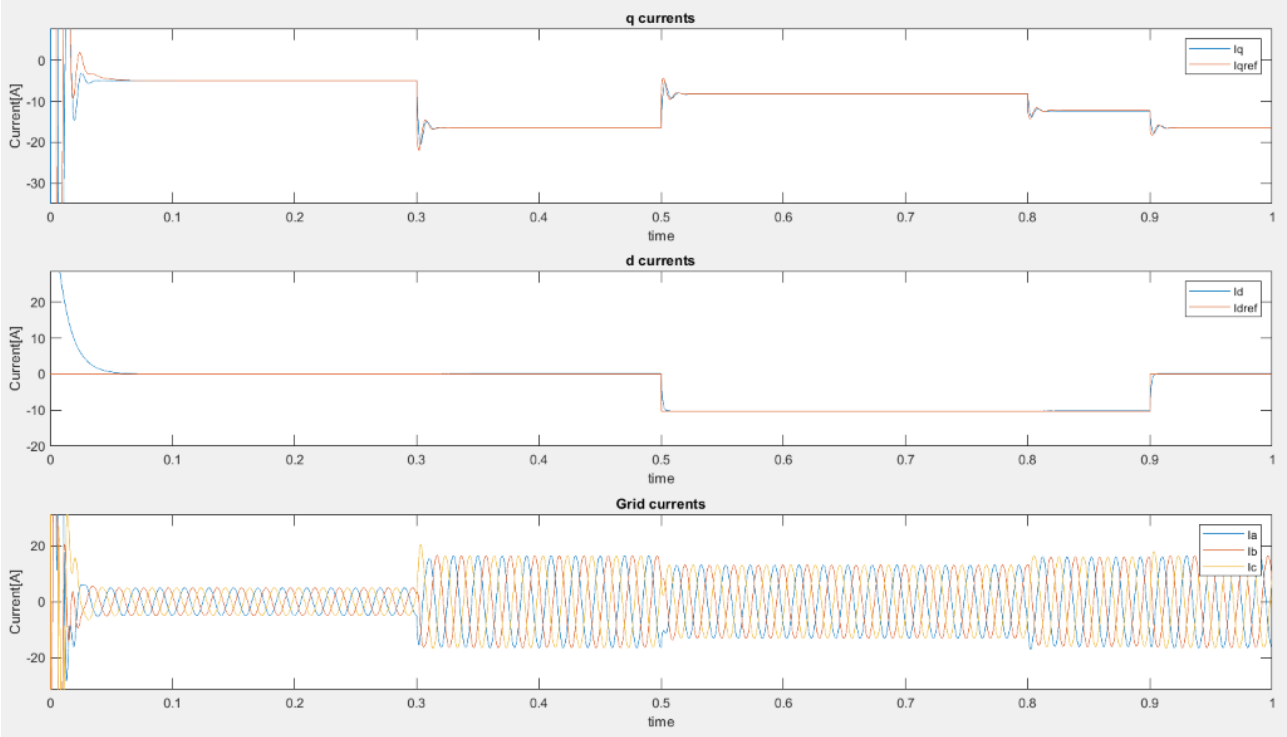

Fig. 23, VSC currents, obtained with MATLAB/Simulink

DC bus voltage

The DC voltage evolution is shown in Fig.23. Each time that DC current changes the voltage controller takes a few milliseconds to regulate the bus voltage to the reference value. The peak Edc voltage is higher for larger injected DC currents.

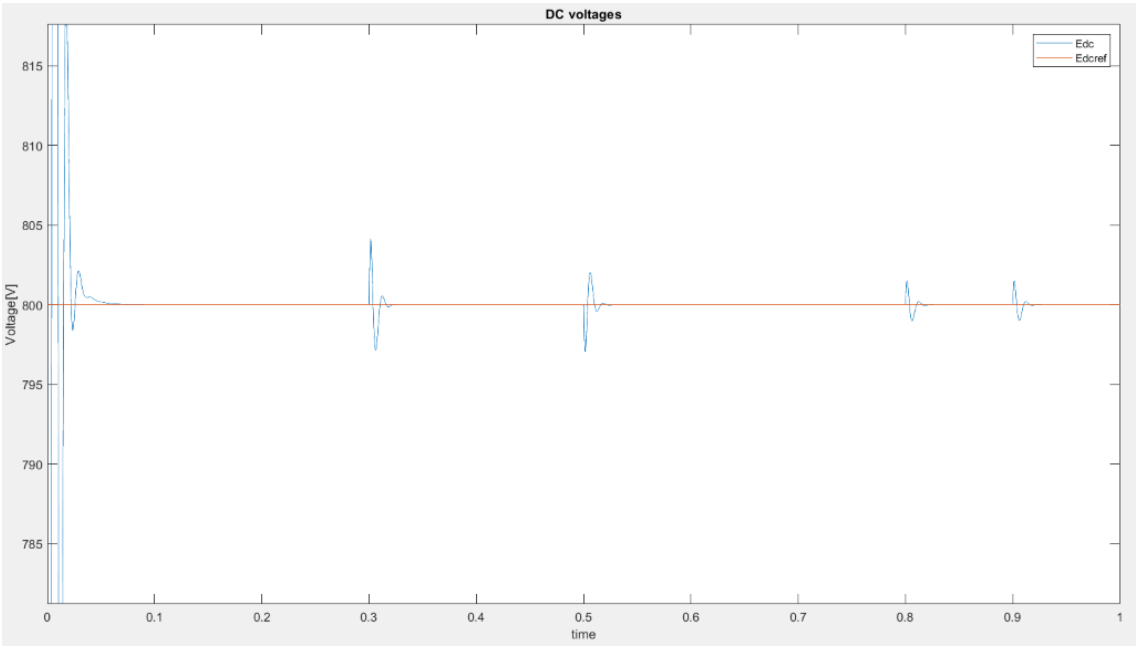

Fig. 24, DC bus measured and reference voltages, obtained with MATLAB/Simulink

Voltages

VSC and the grid voltages both in the qd and abc frame have been obtained in the simulation.

It can be seen how VSC voltages change every time a step in the DC current reference or the reactive power reference is input while the grid voltages measured show constant values equal to $326\ V$ (grid peak voltage) and $Vzd = 0$ (as ensured by the PLL controller).

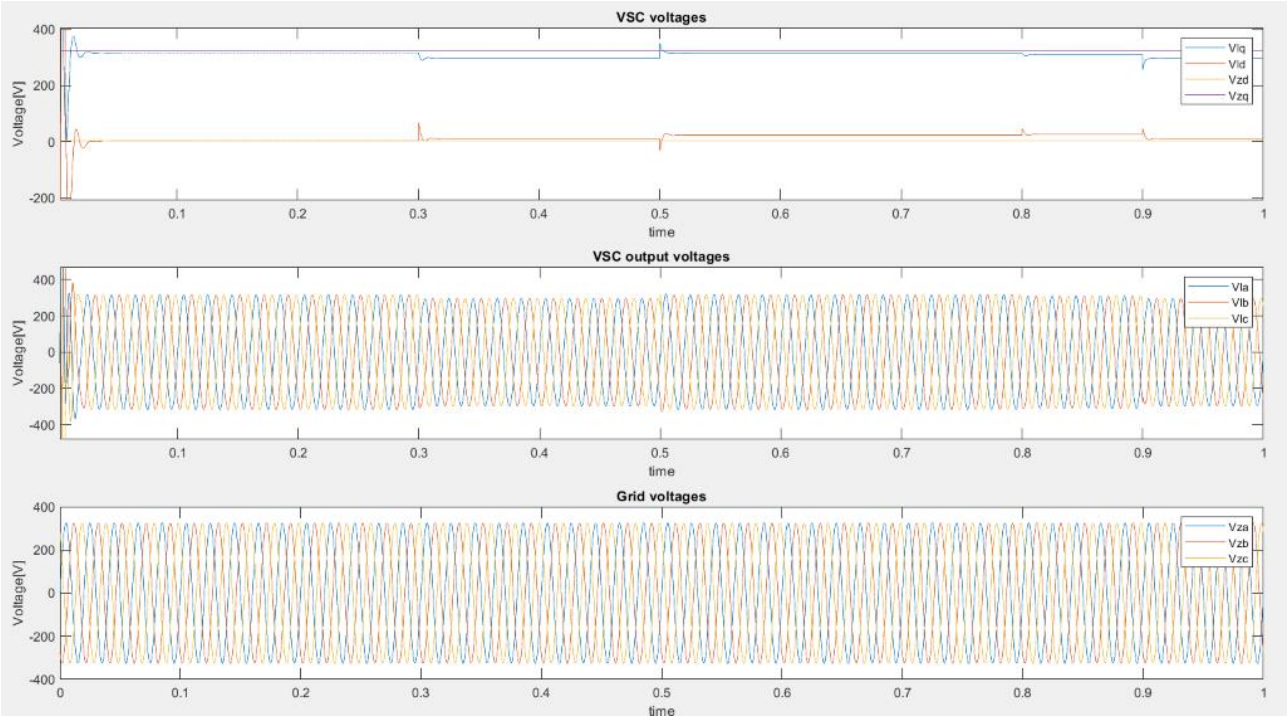

Fig. 25, VSC and grid voltages, obtained with MATLAB/Simulink

5.2.2 Storage system generation

For this test, a battery system of constant DC voltage is assumed (at $800\ V$ like in the previous simulation). Even time constants of the different loops and other parameters for the controller considered are maintained at the same values.

Implementation of the storage system to be interfaced with a VSC can be considered as a simpler case since a DC voltage controller is not needed anymore since now active power reference is simply adjusted to charge the battery or to inject power to the grid depending on the operation of the EMS of the MG or system where the storage system is connected.

Changes in active and reactive power references are done as described in Fig.26.

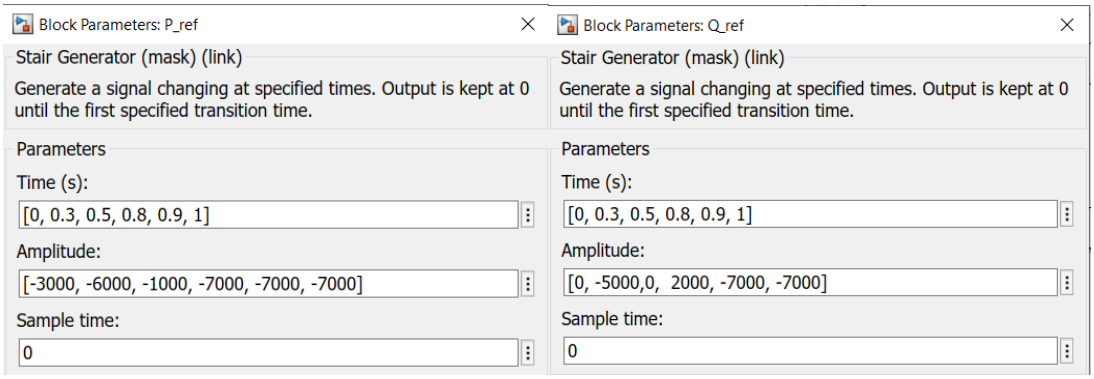

Fig. 26, Input parameters for Pref and Qref

Currents

The currents in the qd frame along with the reference currents and grid currents are plotted in Fig.26. It can be observed the independent control of active and reactive power and how Iq changes each time active power reference change while id follows a trend according to the reactive power reference.

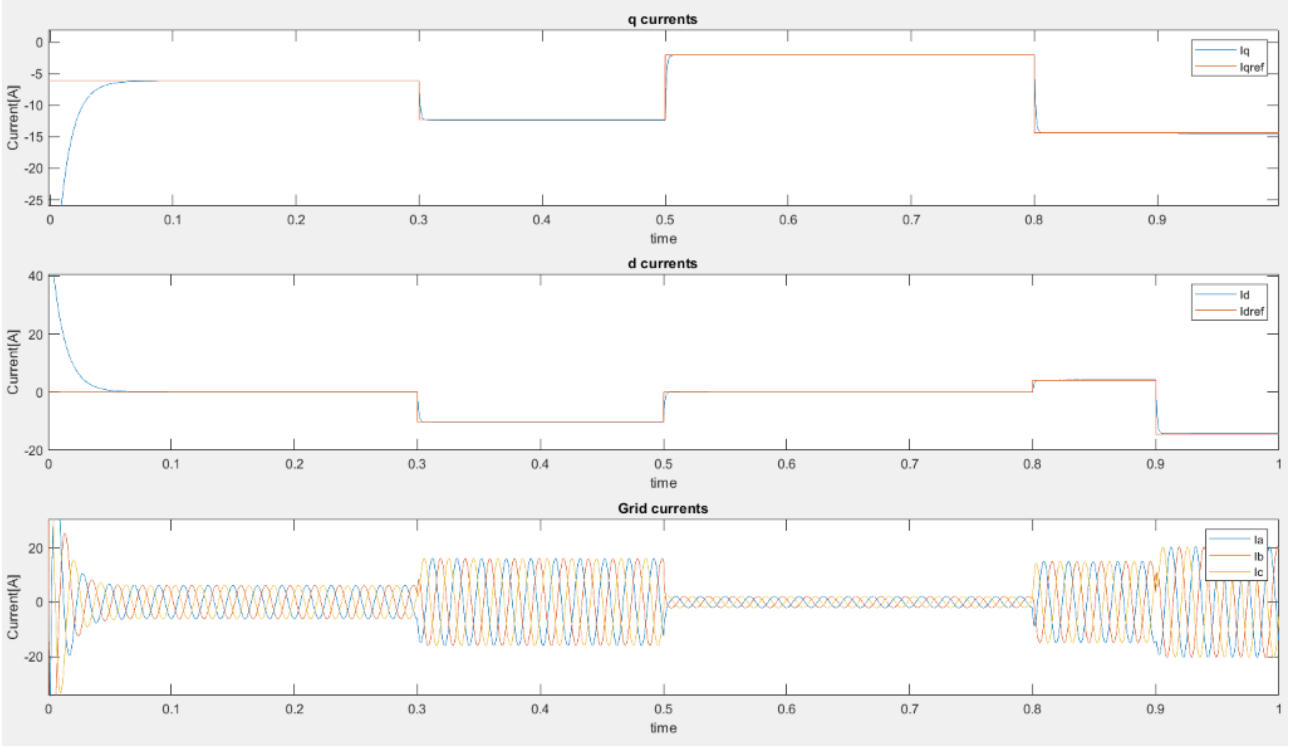

Fig. 27, VSC and grid currents, obtained with MATLAB/Simulink

Voltages

Much like the case for renewable energy generation, measurements for the grid and converter voltages show changes whenever a step is implemented in the input active and reactive power references. It can be noted here too, how Vzd is equal to zero and Vzq to $326V$ (grid peak voltage).

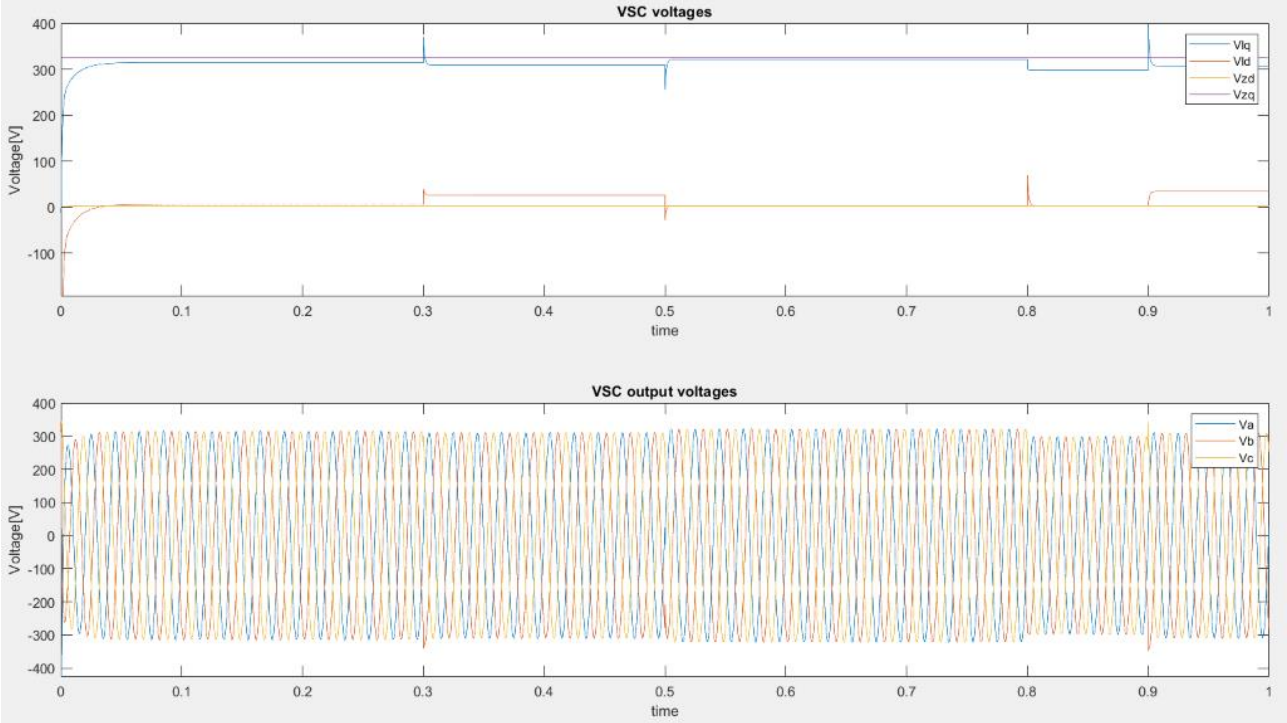

Fig. 28, VSC and grid voltages, obtained with MATLAB/Simulink

Power

Active power increases at $t = 0.3s$ and $t = 0.8s$ and decreases at $t = 0.5s$. The power converter can supply reactive power independently the active power. Between $t = 0.3s$ and $t = 0.5s$ the system is generating reactive power and between $t = 0.8s$ and $t = 0.9s$ the power converter is consuming reactive power.

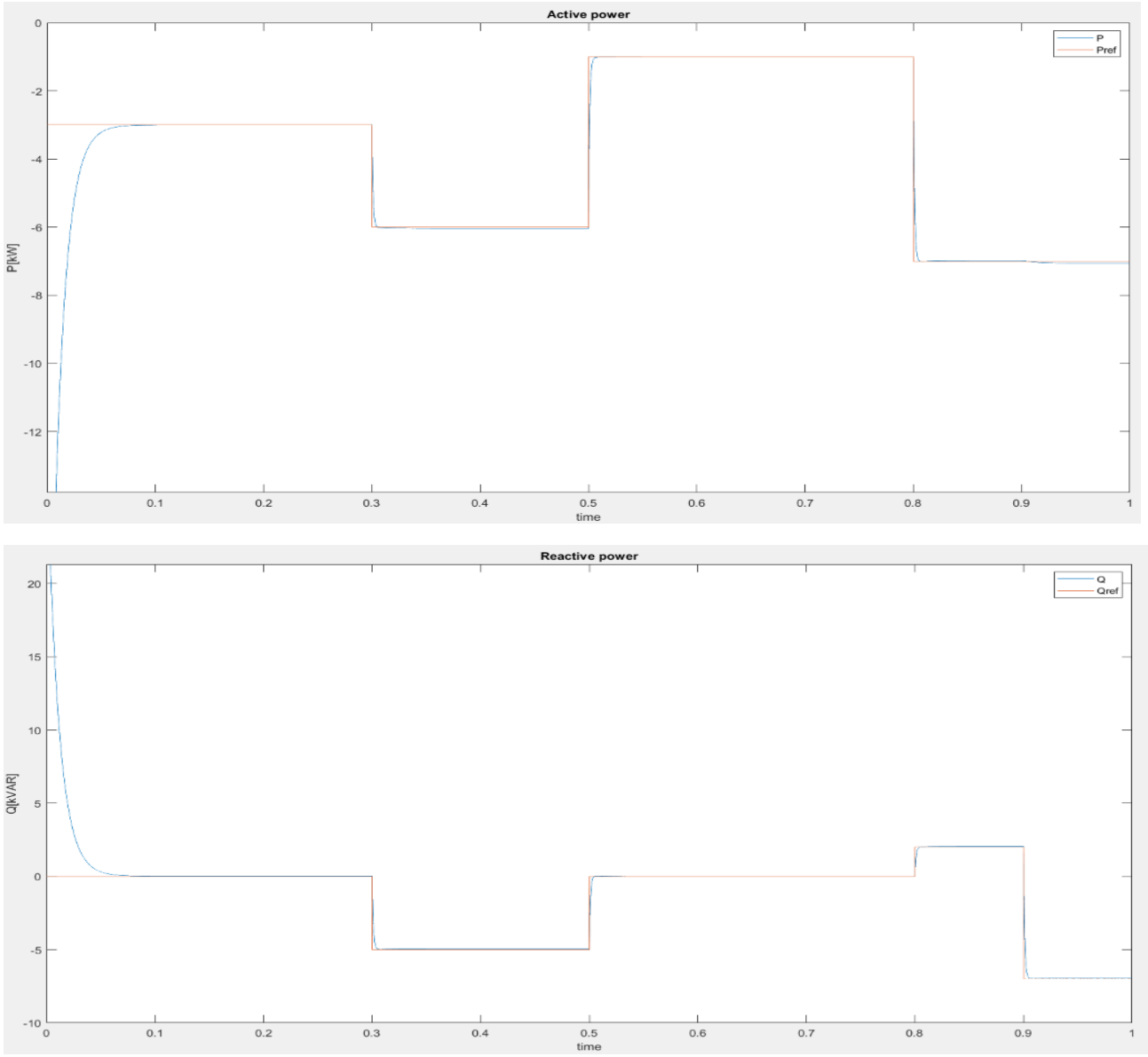

Fig. 29, VSC measured and reference active and reactive power, obtained with MATLAB/Simulink

6. Other Components

6.1 Solar Photovoltaic System

As being the favorite behind-the-meter technology and one of the cheapest source of electrical power in regions with a high solar potential, PV energy production has to be taken into account for providing energy to an autonomous power system such a MG.

MGs that include solar PV as a generating source have the ability to not only provide power when the grid is down, they can also reduce energy costs when the grid is available (Laboratory, 2017).

The complete model of a PV system (comprising the PV Array, the MPPT and DC/DC boost converter) discussed and analyzed in this chapter has been developed mainly following the paper (Snehamoy Dhar, 2015).

All the equations that aim to simulate the behavior of the system different components have been divided and implemented through few fundamental blocks while the only external inputs of the system are the temperature of the cells T_c ,the solar irradiance G and the refence voltage at the DC bus E_{dc}^*.

A simplified PV equivalent circuit with a diode equivalent is employed as model and as said even a maximum power point tracking (MPPT) algorithm has been developed and design in a to maximize power extraction under specified conditions to be injected to the DC bus through a DC/DC converter.

6.1.1 PV Module and Array

To understand the electronic behavior of a solar cell, it is useful to create a model which is electrically equivalent and that is based on discrete ideal electrical components whose behavior is well defined. An ideal solar cell may be modelled by a current source in parallel with a diode; in practice no solar cell is ideal, so a shunt resistance and a series resistance component are added to the model. The resulting equivalent circuit of a solar cell is shown below.

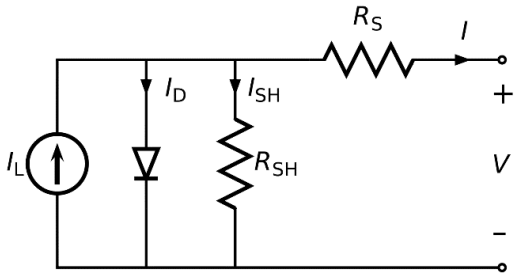

Fig. 30, Equivalent Circuit diagram of the PV model, from (Wikipedia, Solar cell, n.d.)

From the equivalent circuit it is can be seen that the current produced by the solar cell is equal to that produced by the current source, minus that which flows through the diode, minus that which flows through the shunt resistor. It follows the equation:

$$I = I_l - I_d - I_{sh} \qquad eq.25$$

I_l is the light current calculated following the equation:

$$I_l = \frac{G}{G_{ref}} \left[I_{sc} + K_{i,sc} \times (T_c - T_{c,ref} \right] \qquad eq.26$$

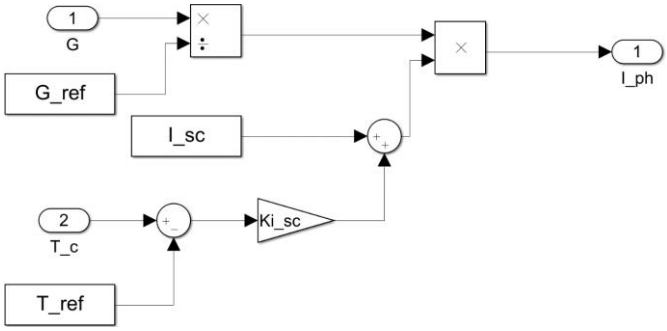

Fig. 31, Light current block, created using MATLAB/Simulink following eq. 26

Where G is the irradiance $[W/m^2]$, G_{ref} the reference irradiance (1000 W/m^2 is used in this study), I_{sc} the short circuit current at the reference conditions (1000 $W/m^2$and 25 °C, provided by the manifacturer), T_c the PV cell temperature (°C), $T_{c,ref}$ the reference temperature (25 °C is used in this study) and finally $K_{i,sc}$ that is the temperature coefficient of the short-circuit current ([A/°C], also provided by the manufacturer);

The equation for the diode direct current is:

$$I_d = I_0 \left[\exp\left(\frac{\frac{1}{T_{c,ref}} - \frac{1}{T_c}}{m\sigma} \right) - 1 \right] \qquad eq.27$$

Where

$$I_0 = I_{0,ref} \left(\frac{T_c}{T_{c,ref}} \right)^3 \exp\left[eE_g \frac{\left(\frac{1}{T_{c,ref}} - \frac{1}{T_c} \right)}{m\sigma} \right] \qquad eq.28$$

$$I_{0,ref} = \frac{I_{sc}}{exp\left[\frac{V_{oc}}{V_t N_s}\right] - 1} \qquad eq.29$$

$$V_t = \frac{\sigma T_c}{e} \qquad eq.30$$

Where I_0 is the reverse saturation current of the diode, $I_{0,\mathrm{ref}}$ the reference reverse saturation current (at reference standard conditions 1000 $W/m^2$and 25 °C), V_t the equivalent voltage for temperature, σ is the Boltzmann constant equal to $1.38 \times 10^{-23}\ J/K$, e theelectron electric charge equal to $1.6 \times 10^{-19}\ C$, m is the diode equality factor equal to 1.2, E_g the bandgap energy of the semiconductor (1.12 eV for the polycrystalline Si at $25°C$), V_{oc} the open-circuit voltage (at reference standard conditions 1000 $W/m^2$and $25°C$, provided by the manifacturer) and eventually N_s is the number of series connected cells in a single PV module (even though the full array will be modelled in series and parallel connected modules too).

The final equation for the current lost flowing through the shunt resistor is:

$$I_{sh} = \frac{V + IR_s}{R_{sh}} \quad eq.31$$

Below represented all the different Simulink blocks

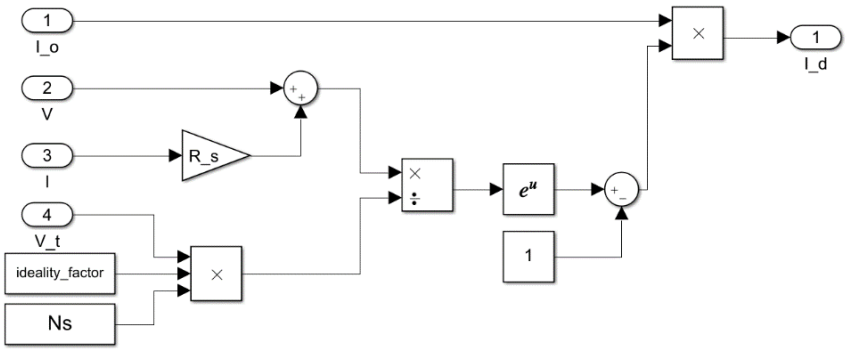

Fig. 32, Diode direct current block created with MATLAB/Simulink following eq.27

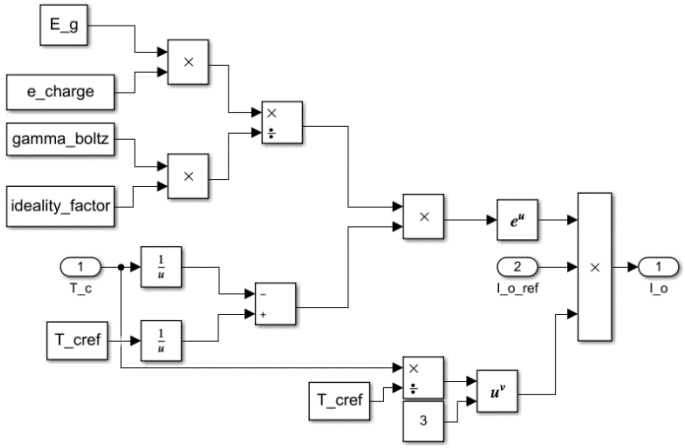

Fig. 33, Reverse saturation current of the diode block, created with MATLAB/Simulink following eq.28

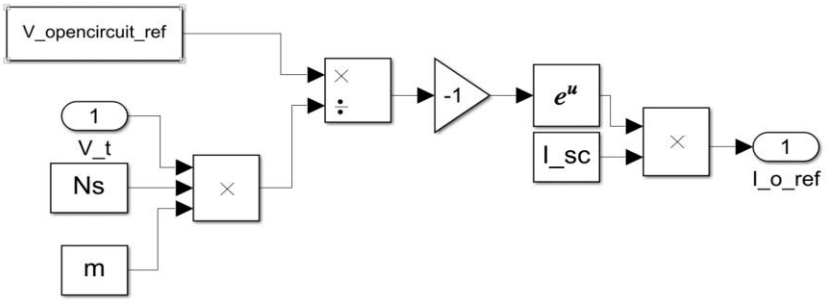

Fig. 34, Reference for the reverse saturation current of the diode block, created with MATLAB/Simulink following eq.29

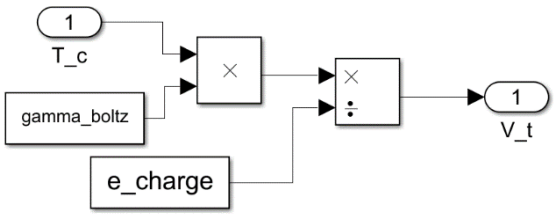

Fig. 35, Equivalent voltage for the temperature block, created with MATLAB/Simulink following eq.30

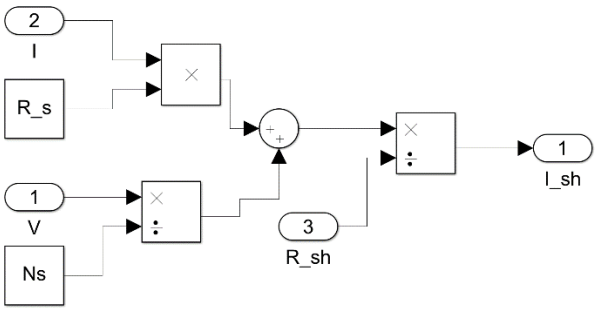

Fig. 36, Current lost flowing through the shunt resistor block, created with MATLAB/Simulink following eq.31

After having modelled all the six different blocks for each equation previously introduced, the final complete model of a PV module (composed by all of them) generates the characteristic curves $V-I$ and $P-I$ for a single module are shown in Fig.38 and 39. To notice that the voltage data points have been generated with a ramp signal (sweep) in order to be able to generate the curves for different temperatures and irradiances.

As it can be observed for higher values than standard condition temperature of $25℃$ and lower values than standard condition irradiance of $1000W/m^2$, performances of the module deteriorate.

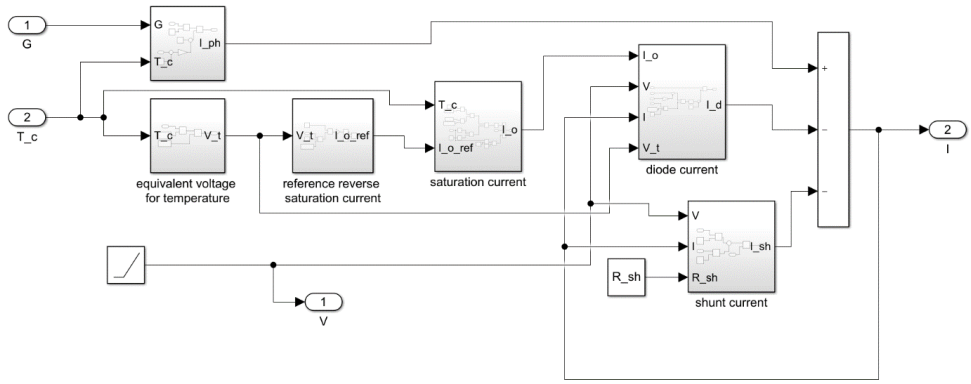

Fig. 37, PV module system created with MATLAB/Simulink following eq. 25

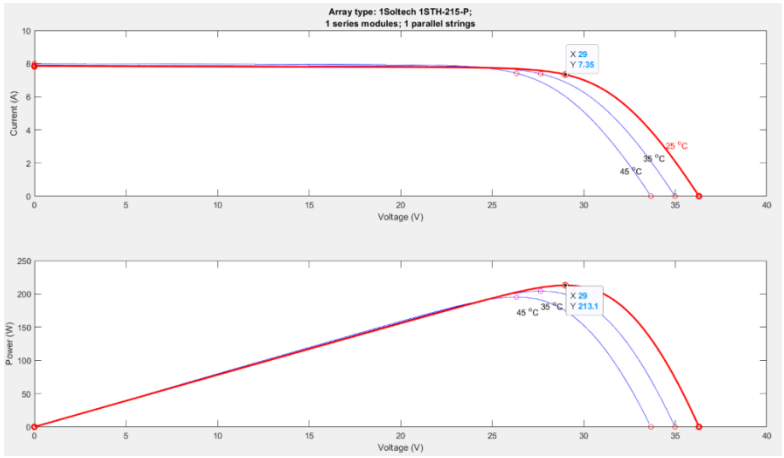

Fig. 38, VI and PV curves for different temperatures created with MATLAB/Simulink

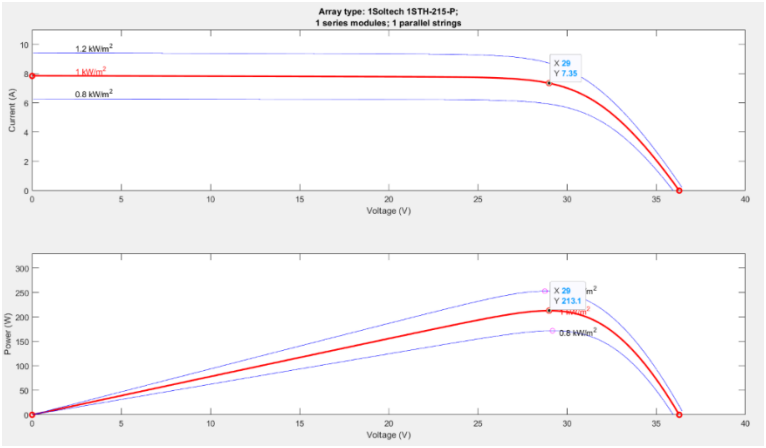

Fig. 39, VI and PV curves for different irradiances created with MATLAB/Simulink

A PV array can be considered and defined as an interconnected system of PV modules that function as a single electricity-producing unit and it consists of PV modules connected in series and in parallel as shown in Fig.40.

The behavioral model of a PV array is very similar to the model of a solar cell or a PV module and can be described by eq.31.

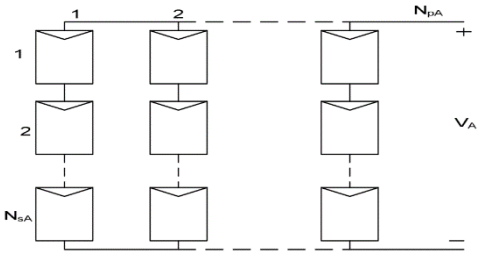

Fig. 40, The connection of modules in a PV array, from (Ahmed, 2010)

$$I = N_p I_l - N_p I_0 \left[exp\left(\frac{\frac{V}{N_s} + \frac{IR_s}{N_p}}{mV_t} \right) - 1 \right] - \frac{\left(\frac{N_p}{N_s}V + IR_s\right)}{R_{sh}} \qquad eq.31$$

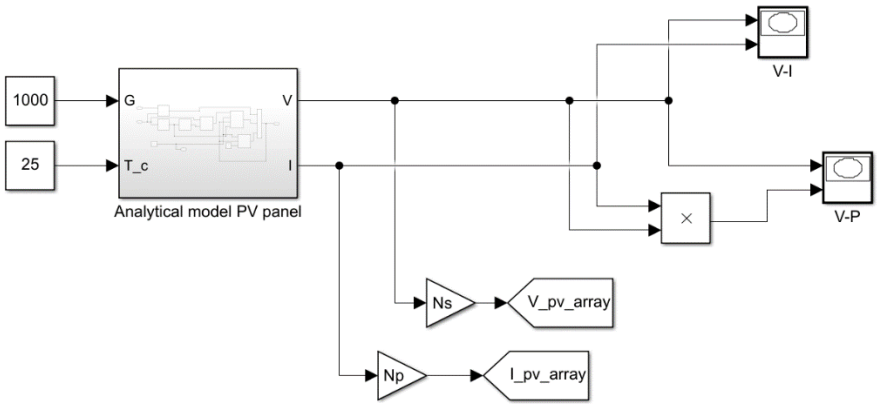

Fig. 41, Complete PV array system, created with MATLAB/Simulink following eq.31

Final values chosen for the simulation to provide the full load (as it will be discussed issues arises in integrating a wind power system within the final microgrid model so that all the power load available will come from the PV system): Ns=6 and Np=1500. Plotted below the curves of such array.

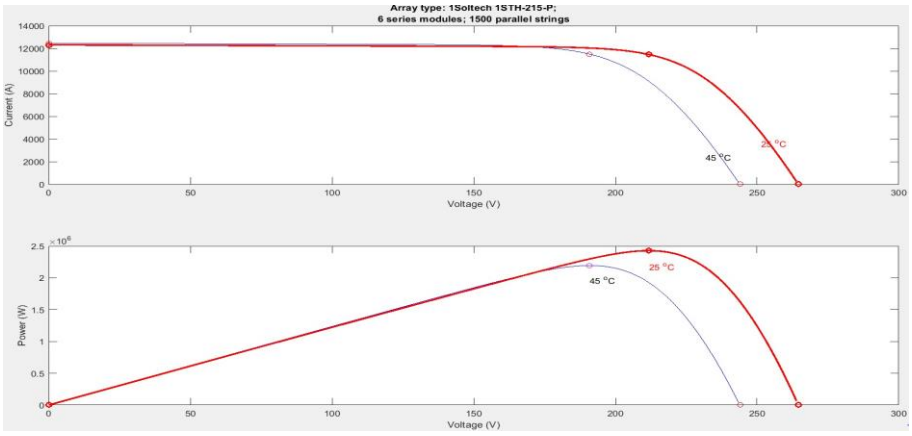

Fig. 42, VI and PV curves for different irradiances created with MATLAB/Simulink

6.1.2 MPPT and DC/DC Converter

DC-DC converter is used to regulate the output DC voltage of PV panels. The regulation is normally achieved by PWM and the switching device consists normally of a MOSFET or IGBT.

MPPT is achieved when the controller algorithm changes and adjusts the duty cycle value (D) of the PWM unit used to generate pulses for the switching device (IGBT or MOSFET as said) of the converter to control the voltage of the array by stepping it up or down.

The Perturb-and-Observe (P&O) technique is an extensively used technique for MPPT and it is implemented for the model. The working principle of this technique is based on the hill-climbing mechanism. Initially, it measures the PV panel output power and then it perturbs the duty cycle of the DC/DC converter, which results in some variation in the output voltage and current and then new power will be calculated. Finally, it compares the new power with the previous power. If the new power is greater than the previous power, then it keeps on repeating the similar change in the duty cycle. However, when it reaches the peak of the hill, then the new power starts decreasing, and it reverses the perturbation process. The power supplied by the PV array after the MPPT is always oscillating around the maximum power (Hill-Climbing concept). Equations 32 and 33 illustrate the mathematical formula for P&O and Fig.43 shows the flow chart of P&O technique.

$$V_{new=}V_{prev} - \Delta V \; if \;\; P_{new} < P_{prev} \qquad eq.32$$

$$V_{new=}V_{prev} + \Delta V \; if \;\; P_{new} > P_{prev} \qquad eq.33$$

where $Vnew$ is the new voltage and $Vprev$ is previous the voltage. Similarly, $Pprev$ is the previous power and $Pnew$ is the new power. ΔV is the achieved voltage change with the change in duty cycle at a step size Δd.

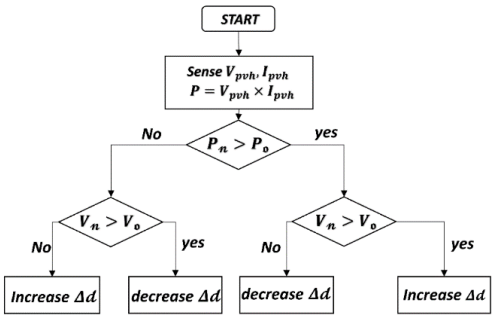

Fig. 43, Flowchart of the P&O technique, from (Muhammad Yaqoob, 2019)

Eventually the complete converter has been modelled using MATLAB/Simulink. It is composed by an inductance in series with the input voltage source, a switch in a parallel branch, a diode in series with the inductance, and one capacitor in the parallel branch (Fig.44). In this case, the switch (consisting in an MOSFET/Diode) is controlled with a PWM technique which can be described by the duty cycle, computed by the MPPT algorithm every Δt (in Fig.45 the operating MATLAB code is shown).

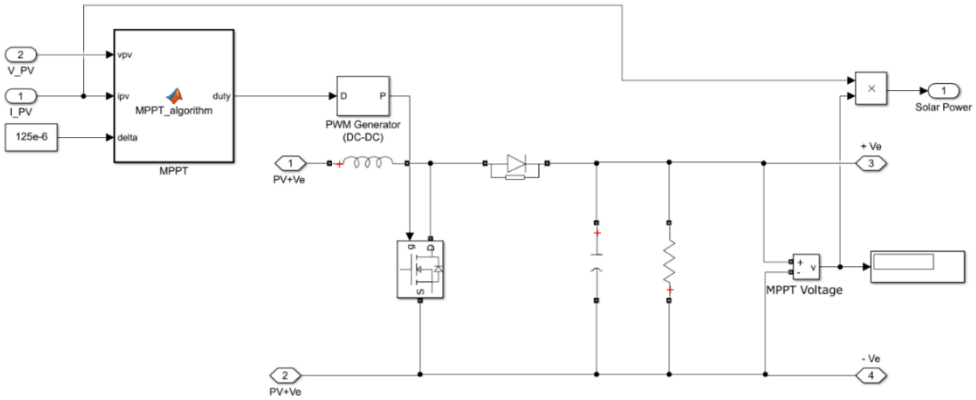

Fig. 44, Boost Converter + MPPT system, created with MATLAB/Simulink

```
function duty= MPPT_algorithm(vpv,ipv,delta)

duty_init = 0.1;

duty_min=0;
duty_max=0.85;

persistent Vold Pold duty_old;

if isempty(Vold)
    Vold=0;
    Pold=0;
    duty_old=duty_init;
end
P=vpv+ipv;
dV= vpv-Vold;
dP= P-Pold;

if P~=0 && vpv>30
   if dP<0
      if dV<0
         duty = duty_old - delta;
      else
         duty = duty_old + delta;
      end
   else
      if dV<0
         duty = duty_old + delta;
      else
         duty = duty_old - delta;
      end

if duty>=duty_max
    duty=duty_max;
elseif duty < duty_min
    duty=duty_min;
end

duty_old=duty;
Vold=vpv;
Pold=P;
```

Fig. 45, MPPT code for duty cycle computation created with MATLAB

Parameter chosen for the DC/DC converter are: the inductance L=0.05 mH, the resistance of the diode $Ron = 0.001\ \Omega$, its inductance $Lon = 0\ H$, forward voltage $Vf = 0.8\ V$ and snubber resistance $Rs = 500\ \Omega$ and finally snubber capacitance $Cs = 250\ nF$. For the MOSFET the resistance $Ron = 0.1\ ohm$, the internal diode resistance $Rd = 0.01\ \Omega$ and inductance $Lon = 0\ H$ and snubber resistance Rs=100 $m\Omega$. Finally, the capacitor and the resistor in the parallel branch present values of $C = 550\ mF$ and $R = 20\ \Omega$, respectively.

6.2 Wind Power System

A wind power system to be included in the final model of the MG system has been modelled. For areas with even modest wind resources, adding wind generation to a LV MG increases the renewable energy supply fraction, reduce back-up generator operation or fuel consumption, and potentially increasing storage system life (WindPower, 2019). Wind turbines operate at night, during rainy seasons, and in the winter, supplementing available solar energy. More renewable energy, less fuel and less energy cycled through the battery.

In order to extract the maximum power of wind with fluctuating speed, different turbine speeds are needed (El-Saadany, 2012). In order to cope with this conflict, Doubly Fed Induction Generator (DFIG) is commonly used because DFIG can be controlled to maximize the extracted energy while using a converter with lower rating in comparison to synchronous generators interfaced by a full back-to-back converter. These benefits with the capability of providing reactive power result in the preference of using DFIG among other generator types.

This concept of the machine is as an alternative to more common asynchronous and synchronous machines. It can be advantageous in applications that have a limited speed range, allowing a reduction in the size of the supplying power electronic converter as, for instance, in variable-speed generation.

The model of the DFIG generator and the back-to-back AC/DC/AC converter and its control have been designed using MATLAB/Simulink and it has been developed following mainly three papers: (Iwanski, 2014), (G. Abad, 2011) and (G. Abad, Back-to-Back Power Electronic Converter, 2011)

The typical supply configuration of the doubly-fed-induction machine (DFIM) is shown in Fig.46. The stator is supplied by three-phase voltages directly from the grid at constant amplitude and frequency, creating the stator magnetic field. The rotor is also supplied by three-phase voltages that take a different amplitude and frequency at steady state in order to reach different operating conditions of the machine (speed, torque, etc.). This is achieved by using a back-to-back three-phase converter, as represented in the simple schematic in the figure. This converter, together with the appropriate control strategy, is in charge of imposing the required rotor AC voltages to control the overall DFIM operating point and to perform the power exchange through the rotor to the grid. Although a VSC is shown, different configurations or converter topologies could be utilized.

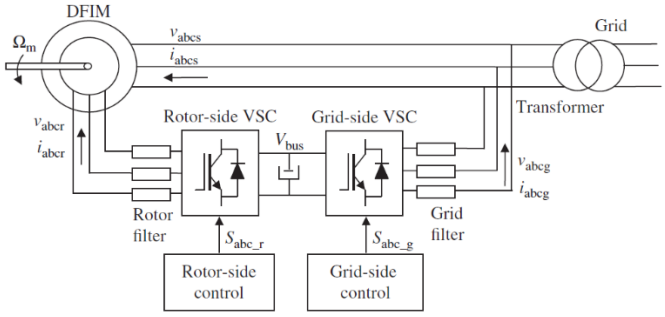

Fig. 46, General supply configuration of DFIM, from (Iwanski, 2014)

As it can be seen from the schematic of the system above, control of both rotor-side and grid-side converter will be implemented for ultimately control the doubly fed induction machine (DFIM).

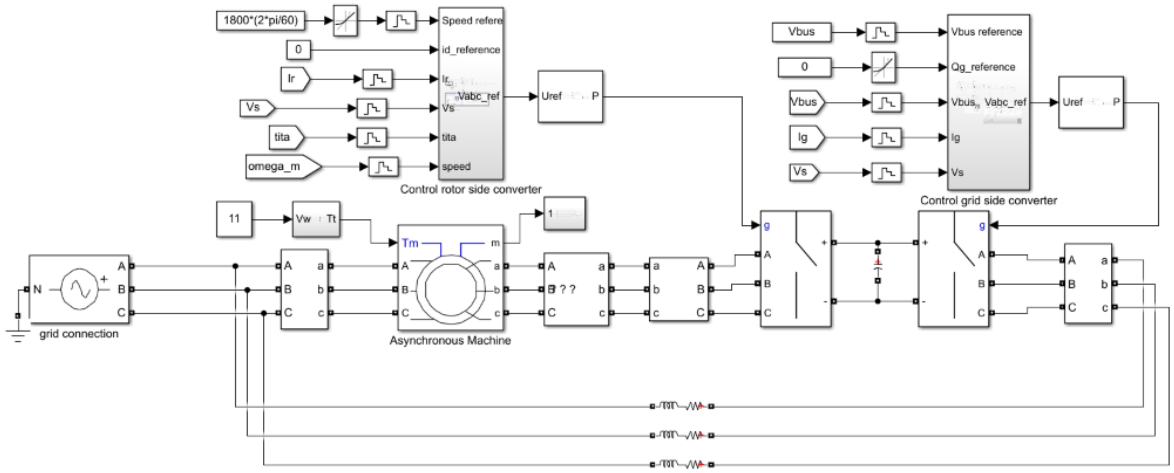

Fig. 47, Complete DFIG-based wind power system, created with MATLAB/Simulink

The VSCs implemented in the system is a Simulink Universal bridges block with ideal switches as power electronic device which are controlled by means of PMW (via a 2-levels PMW generator). Parameters of the system are: the stator frequency fs equal to $50\ Hz$, the rated stator power Ps equal to $1\ Mw$, Rated rotational speed ωm equal to $1500\ rpm$, the stator rated voltage Vs equal to $400\ V$ (same as grid voltage having direct connection with this), the rated stator current Is equal to $1760\ A$, the rated torque Tem of the machine equal to $12732\ Nm$, stator/rotor turns ratio u equal to $1/3$ and finally the rated rotor voltage Vr equal to $2070\ V$.

6.2.1 Components

The wind turbine

A three-blade wind turbine has been modelled and implemented for the wind power system. Parameters considered are: the blades radio $R = 42\ m$, air density $\rho = 1.225\ kg/m^3$ and gearbox ratio $N = 100$. Torque coefficient Ct curve in function of the tip speed ratio $\boldsymbol{\lambda}$ (eq.37) and power curve in function of the wind speed are shown below, showing a rated power of the wind turbine of $Pt = 1\ MW$.

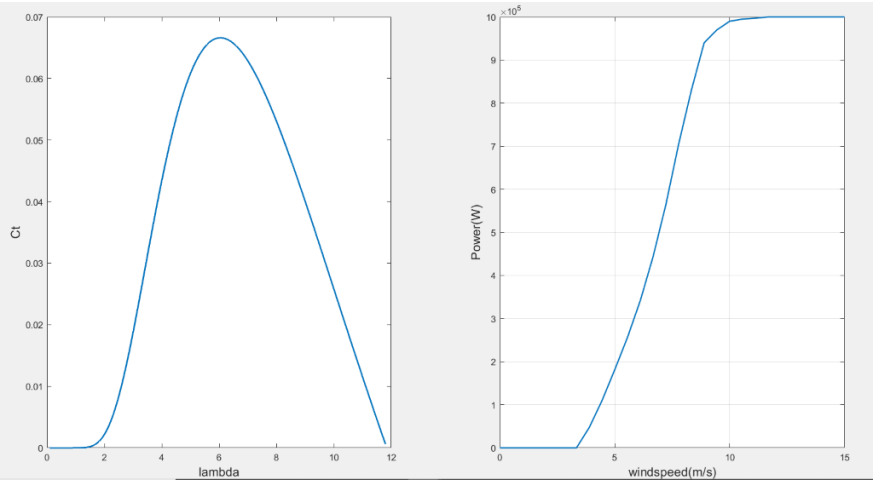

Fig. 48, Ct in function of λ and P in function of Vw, created with MATLAB

The aerodynamic model represents the power extraction of the rotor, calculating the mechanical torque as a function of the air flow on the blades. The wind speed can be considered as the averaged incident wind speed on the swept area by the blades with the aim of evaluating the average torque in the low speed axle.

The torque generated by the rotor is defined by the following expression:

$$T_t = \frac{1}{2}\rho\pi R^3 V_w^2 C_t \qquad eq.34$$

As mentioned in a previous section, the most straightforward way to represent the torque and power coefficient Cp is by means of analytical expressions as a function of $\boldsymbol{\lambda}$ and the pitch angle (β). One expression commonly used, and easy to adapt to different turbines, is

$$C_p = k_1\left(\frac{k_2}{\boldsymbol{\lambda}_i} - k_3\beta - k_4\beta^{k_5} - k_6\right)\left(e^{k_7/\lambda_i}\right) \qquad eq.35$$

with the tip step ratio,

$$\lambda_i = \frac{1}{\lambda + k_8} \qquad eq.36$$

and

$$C_t = \frac{C_p(\boldsymbol{\lambda})}{\boldsymbol{\lambda}} \qquad eq.37$$

Here represented a schematic of the wind turbine modelled using MATLAB/Simulink according to eq.34 with input wind speed Vw, rotational speed ω_m and radio R, giving the torque of the three-blade wind turbine as output.

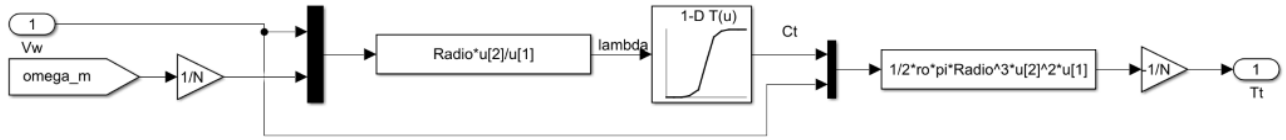

Fig. 49, Turbine model block, created with MATLAB/Simulink

As for the control strategy of the DFIG, more specifically the MPPT strategy, between the ones proposed in (Iwanski, 2014), one of the simplest has been chosen. It is called Indirect speed control.

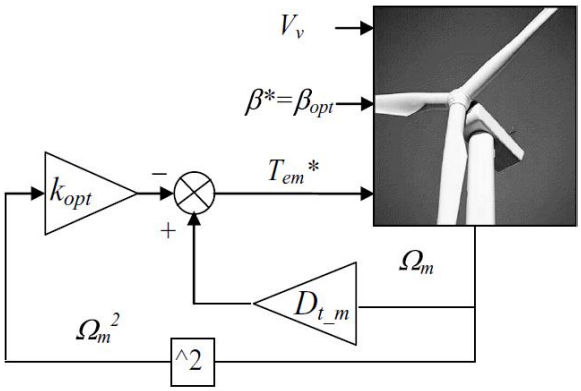

Fig. 50, Indirect speed control, from (G. Abad, 2011)

As a very small value of the damping coefficient of the mechanical system has been considered, it results in an optimal torque simply evolving as a quadratic function of the wind turbine speed. $Kopt$ has been computed according to the eq.38.

$$k_{opt} = \frac{1}{2}\rho\pi\frac{R^5}{\lambda_{opt}^3 N^3}C_{pmax} \qquad eq.38$$

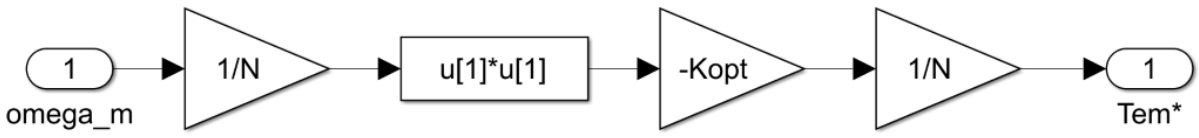

Fig. 51, Indirect speed control giving as output the optimal torque reference, created with MATLAB/Simulink

As it can be noted from Fig.57, this control strategy replaces a simple speed PI controller previously implemented to first test the correct functioning of the Rotor Side Converter control (RSC).

The Rotor side converter

The control strategy for the DFIG implemented is based on a vector control strategy performed in a synchronously rotating dq frame, in which the d-axis is aligned, in this case, with the stator flux space vector, as illustrated in Fig.52.

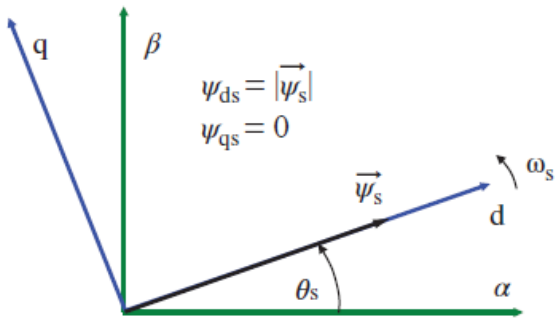

Fig. 52, Synchronous rotating dq reference frame aligned with the stator flux space vector from (Iwanski, 2014)

Owing to this alignment choice, it will be shown that the direct rotor current is proportional to the stator reactive power, and that the quadrature rotor current is proportional to the torque or active stator power. And once again in (Iwanski, 2014), it is demonstrated that it is possible to perform dq rotor currents control, simply by using a regulator for each current component, as shown in Fig.53.

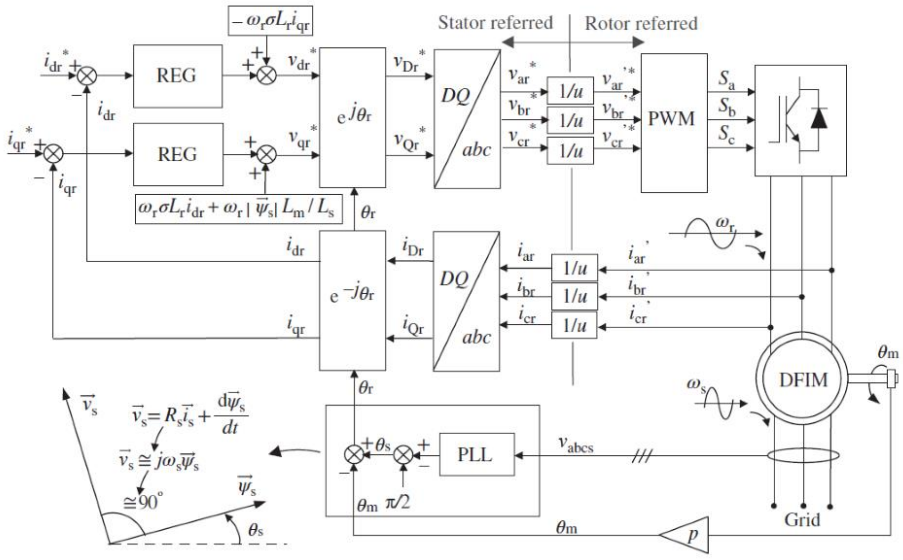

Fig. 53, Current control loops of the DFIM, from (Iwanski, 2014)

For getting the angle of the stator three-phase voltages it has been implemented a $\alpha\beta$ transformation, and from having this voltages in stationary reference frame instead of a PLL a simple $atan$ Simulink block function has been used for then subtracting 90 degrees to get the final stator angle θ_s. The rotor angle θ_r is finally obtained from the stator angle minus θ_m, angle of the machine shaft.

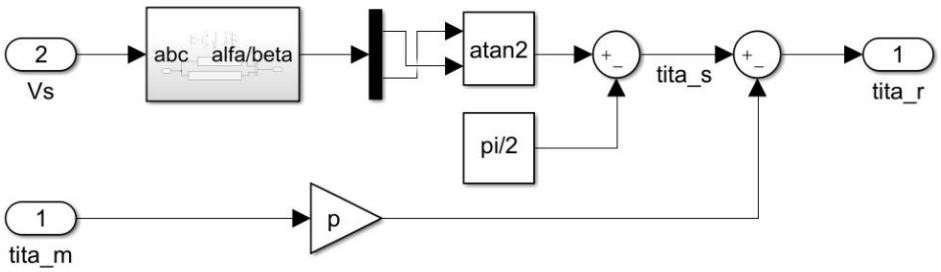

Fig. 54, Computation of the rotor angle, created with MATLAB/Simulink

So that wo different regulators deploying PI controllers are used for Iqr and Idr. As can be seen again from the scheme proposed in Fig.53, after this step, for finally obtaining the two reference voltages Vdr and Vqr a cancellation of coupling terms (as shown in eq.39 and 40) is necessary.

$$v_{dr} = R_r i_{dr} + \sigma L_r \frac{d}{dt} i_{dr} - \omega_r \sigma L_r i_{qr} + \frac{L_m}{L_s} \frac{d}{dt} |\psi_s| \qquad eq.39$$

$$v_{qr} = R_r i_{qr} + \sigma L_r \frac{d}{dt} i_{qr} + \omega_r \sigma L_r i_{dr} + \omega_r \frac{L_m}{L_s} \frac{d}{dt} |\psi_s| \qquad eq.40$$

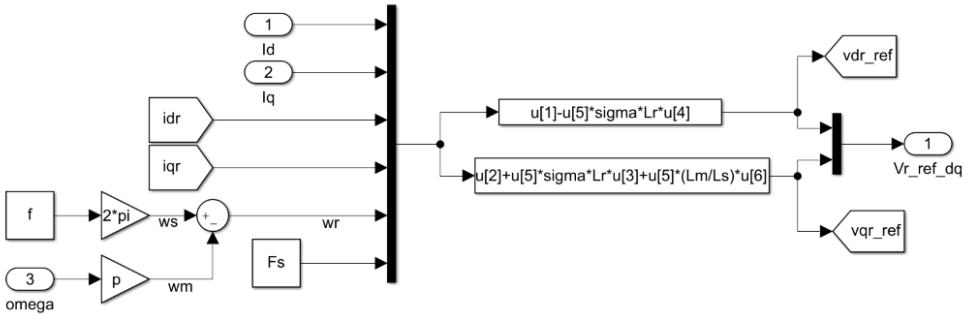

Fig. 55, Decoupling terms block for the RSC control created with MATLAB/Simulink

Once current loops have been concluded a speed regulator loop has been added (reactive power compensator and regulator has not been considered, for simplicity as Id reference has been set to zero from the start).

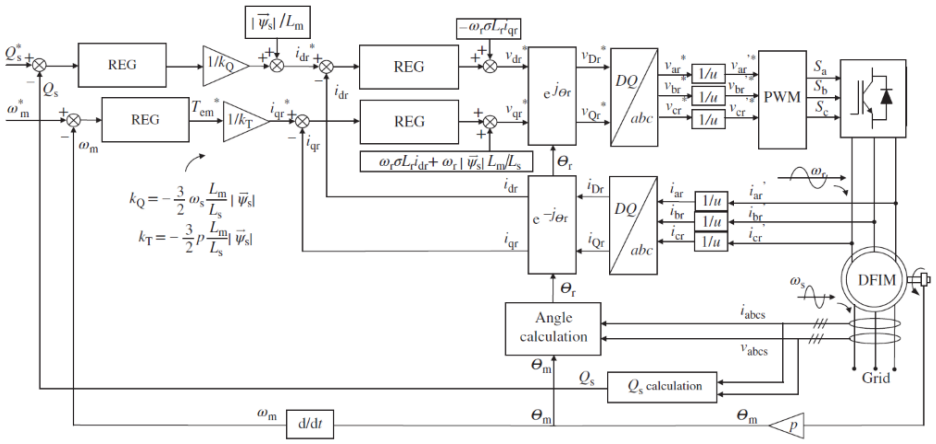

Fig. 56, Complete vector control of the DFIM with the current loops introduced before, a speed loop (to control speed of the shaft of the machine and a stator reactive power loop, from (Iwanski, 2014)

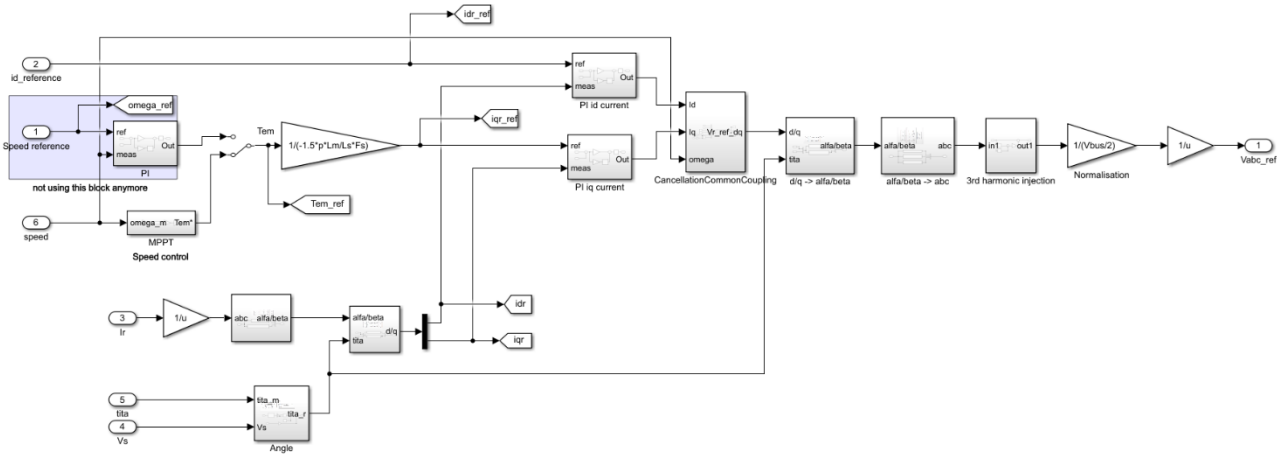

Fig. 57, RSC complete control system diagram, created with MATLAB/Simulink

The PMW block uses triangular waveform normalized 1 this output needs to be normalized to the Vdc bus at the converter with a gain as shown in the Fig.57. A 3rd harmonic injection block has been implemented too as it allows for an increase of around 15 % of the input voltage.

The grid side converter

The grid-side-converter (GSC) is in charge of controlling part of the power flow of the DFIM. The power generated by the wind turbine is partially delivered though the rotor of the DFIM as advanced in this paragraph. This power flow that goes through the rotor flows also through the DC link and finally is transmitted by the grid side converter to the grid Introduction of inductive filter to interface GSC to the grid.

In order to operate with the grid and rotor side converters with real voltages it is necessary to introduce an ideal transformer to implement the stator and rotor relation (rotor voltage is three times the stators').

An identical PMW modulator already used for the RSC has been implemented.

The grid voltage-oriented vector control (GVOVC) block diagram is shown in Fig.58 where it shown how, once grid voltages and currents are measured, control will be operated on the DC bus voltage (set to $1150V$) and on the reactive power exchanged with the grid.

Control of $Vbus$ is necessary since the DC link is mainly formed by a capacitor. Thus, the active power flow through the rotor must cross the DC link and then it must be transmitted to the grid. Therefore, by only controlling the $Vbus$ variable to a constant value, this active power flow through the converters is ensured, together with a guarantee that both grid and rotor side converters have available the required DC voltage to work properly.

Therefore, the GVOVC block diagram is shown below. From the $Vbus$ and Qg references, it creates pulses for the controlled switches Sa_g, Sb_g, and Sc_g.

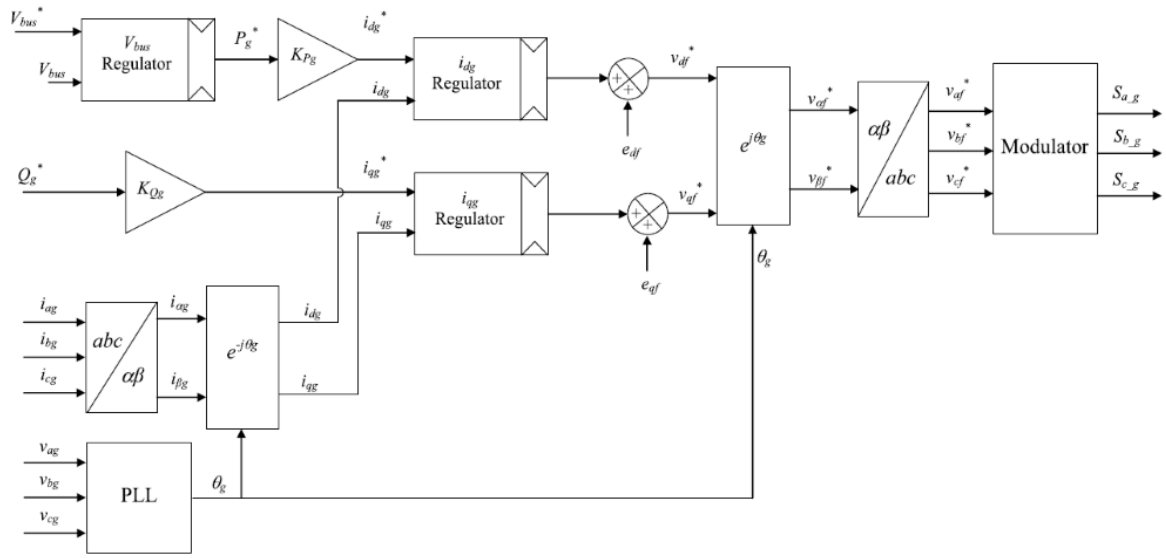

Fig. 58, GVOVC diagram, from (G. Abad, Back-to-Back Power Electronic Converter, 2011)

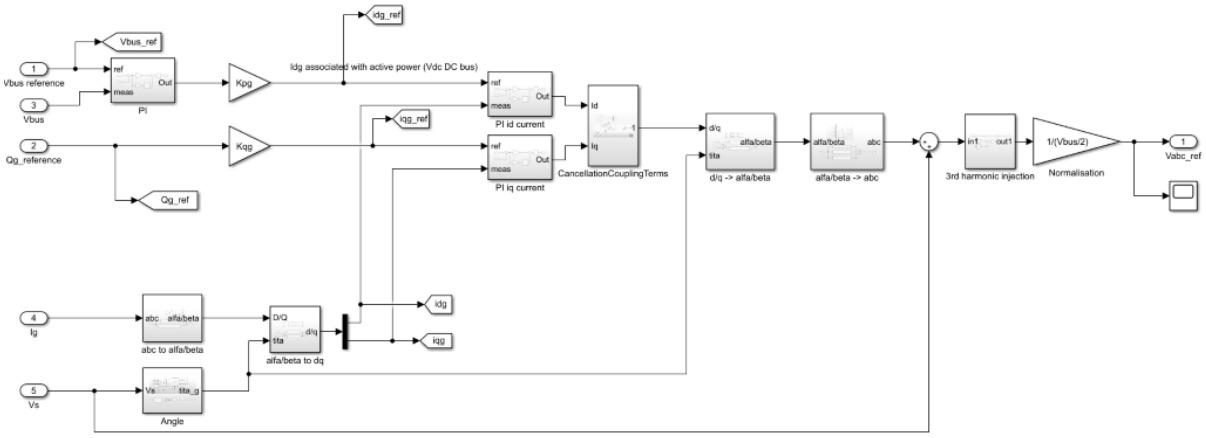

Fig. 59, GSC complete control system diagram, created with MATLAB/Simulink

The angle θ_g of the grid voltage is estimated (much like for the control of the RSC, through a simple $atan$ function) and measured grid current Ig is transformed. The DC bus Voltage Vdc is controlled using a PI regulator. Then, the dq voltage references (vdf , vqf) are independently created from the dq currents (idg, iqg) controllers.

$$v_{df} = R_f i_{dg} + L_f \frac{di_{dg}}{dt} + v_{dg} - \omega_s L_f i_{qg} \qquad eq.40$$

$$v_{qf} = R_f i_{qg} + L_f \frac{di_{qg}}{dt} - \omega_s L_f i_{dg} \qquad eq.41$$

There is also one coupling term in that is best considered in the control as a feed-forward term (at the output of the current controllers). So that for better performance in the dynamic responses it has been implemented a decoupling term block, for the final computation of the voltage references to be sent to the PMW modulator. Terms that can be seen added in Fig. 58 are expressed by eq. 42 and 43.

$$e_{df} = -\omega_s L_f i_{qg} \qquad eq.42$$

$$e_{qf} = \omega_s L_f i_{dg} \qquad eq.43$$

Fig. 60, Decoupling terms block for the GSC control created with MATLAB/Simulink

6.2.2 Simulation results

Before showing main findings of the simulations performed, it is worth mentioning that the start-up of the turbine is done with direct connection to the stator of the machine, while in reality it should be made differently since this causes significant transient and overshoots of currents in both rotor and stator parts of the machine and torque values (that can be observed in every graphs obtained in the simulation). But for simplicity purposes all elements have been started at the same time, so that focus will be only put on analyzing the system variables once a ''steady state'' is reached. With a hypothetical instantaneous changed in wind speed from $7m/s$ to $11\ m/s$ operated at $t = 3.6s$ it can be noted how rotational speed and torque (in absolute value, as the machine is working as a generator) increase, i.e. generated power increases. Current Iq shows a rising trend as well. Graphic shows there is correspondence between torque and current Iq evolution, with this being properly controlled to respective references, while Id is maintained to zero (reference is set to a null value).

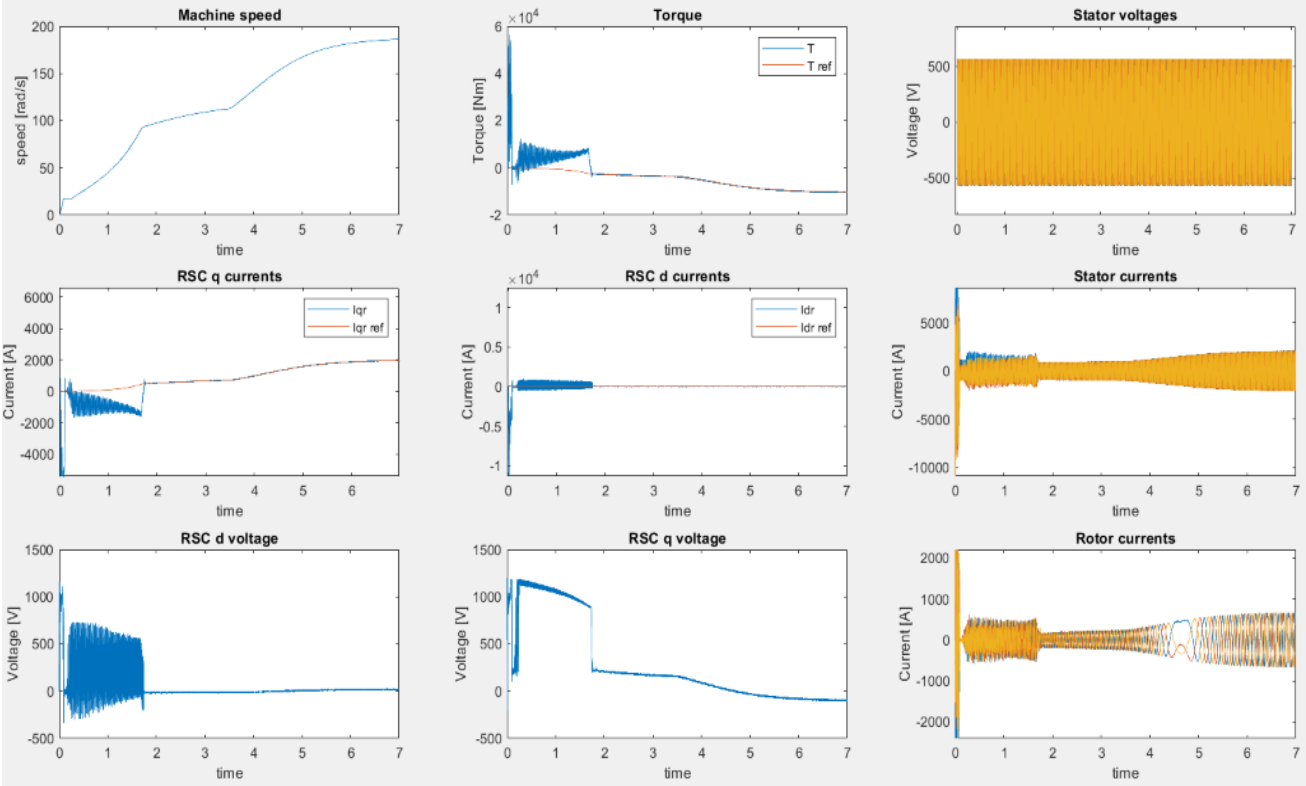

Fig. 61, Rotor side currents and voltages, obtained from MATLAB/Simulink

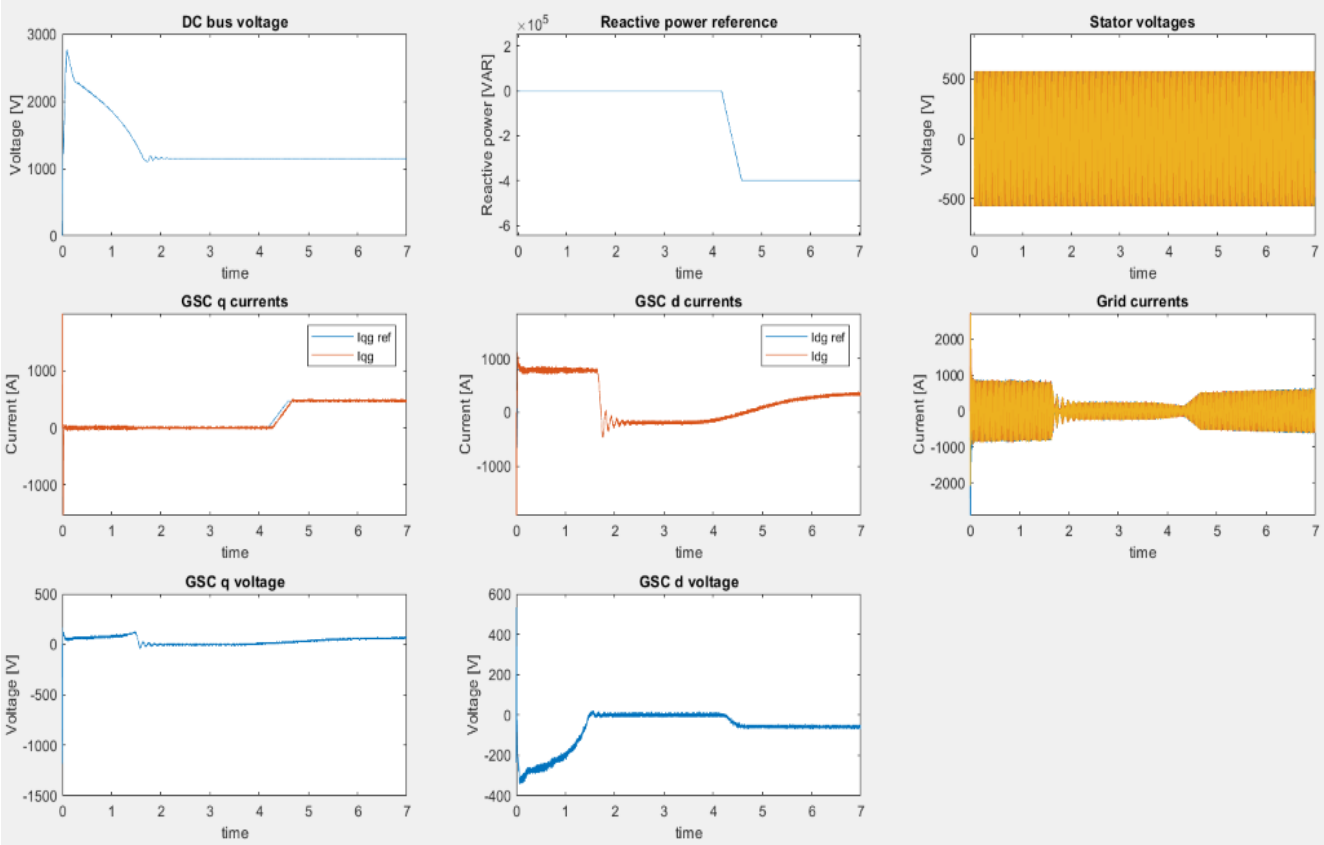

Fig. 62, Grid side currents and voltages, obtained from MATLAB/Simulink

Once again even for the GSC, it is worth to mention the big overshoot happening in the controlled DC Bus voltage Vdc (as said, this is due to the ''strong'' and unconventional start-up that is operated), reaching steady state at around $t = 2s$ in the simulation.

There is correspondence timewise between the behavior of the GSC and RSC for the controlled currents to reach a steady-state evolution.

Voltages values present very small values as in the control diagram, since a feed-back grid voltage has been used in this. When the change in wind speed is operated at $t = 3.6s$ a perturbation is caused in the bus voltage. As Idg is associated with the active power, this starts rising too.

As a change in the reactive power reference $Qref$ from a null value to one equal to $400VA$ is input at the GSC control block at $t = 4.31s$ even current Iqg modifies significantly, simultaneously with the grid current Ig.

As speed and torque increase by means of the MPPT control working to its optimum rotational speed value according to the wind speed that has been set, current and torque loops show proper functioning.

6.3 Storage system

The energy storage system (ESS) is an essential part of a power system like a MG because it is analogous to the spinning reserve of large generators in a conventional grid. It ensures the balance between energy generation and consumption especially during abrupt changes in load or generation being able, for instance, to store energy at off-peak hours and supply energy at peak hours. In some cases, it can regulate real and reactive power quality in an electric distribution system.

However, existing ESS technology faces challenges in storing energy due to various issues, such as charging/discharging, safety, reliability, size, cost, life cycle, and overall management. Thus, an advanced ESS is required with regard to capacity, protection, control interface, energy management, and characteristics to enhance the performance of ESS in MG applications

Since many of the issues listed above are out of the scope for this project, a very simplified model of an ESS and all its components (the battery and the bidirectional DC/DC converter which charge and discharge the battery at the required voltages) have been modeled using the own knowledge of the author about power electronics and storage systems.

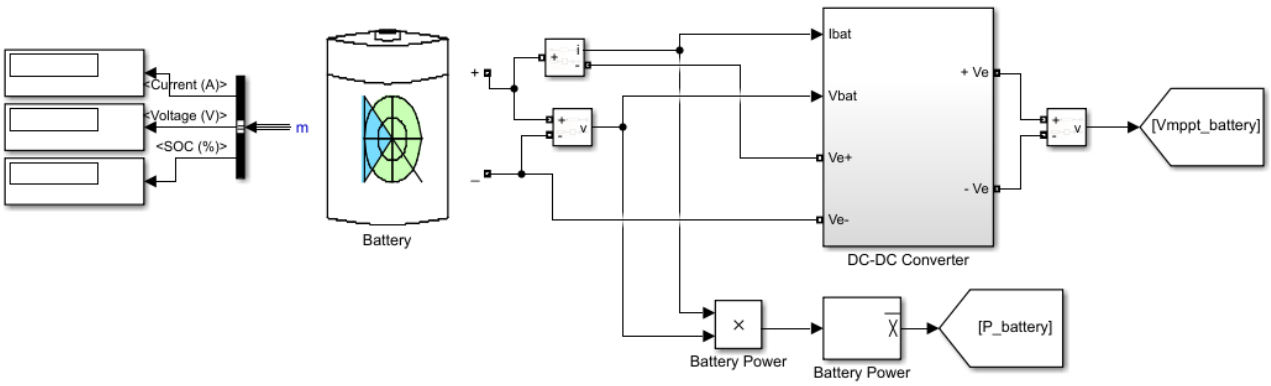

Fig. 63, Complete ESS, created with MATLAB/Simulink

Battery is the key element that supplies power to the system when the loads have peak values and the power provided by the DRs present in the distribution system is not sufficient to cover them. Batteries are complex electrochemical elements and their mathematical modeling is completely out of the scope of this project, so that a preset Simulink model of a battery is used, as it can be seen from Fig.64.

Parameters chosen are rated voltage equal to $200\,V$, rated capacity of $900\,Ah$ (for the sizing a simple calculation has been made for having $200\,kWh$ of power)

A fundamental part of the system is the DC/DC boost converter. This is modelled similarly to the one deployed for the solar PV system as shown in Fig.65 (it consists of an inductance in series with the input voltage source, a switch in a parallel branch, a diode in series with the inductance, and one capacitor in the parallel branch). Even in this case, it is used a simple P&O technique based on the hill-climbing mechanism for MPPT.

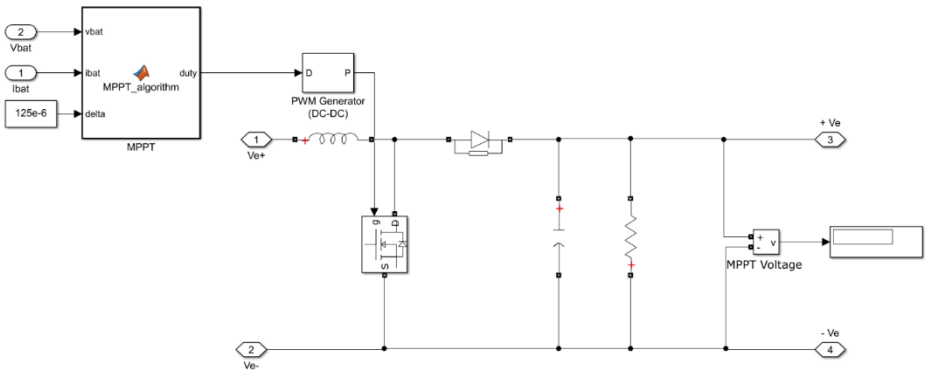

Fig. 64, Boost Converter + MPPT system, created with MATLAB/Simulink

Parameters for the DC/DC converter are alike the ones used for the PV system except for: resistance $R = 1\ \Omega$ and series inductance $L = 0.05\ \mu F$.

7. Microgrid

7.1 Procedure and Model

In this chapter a finalized model of the MG is presented. As already mentioned In Chapter 6, since a proper start-up of the wind power system resulted too difficult to implement, this will not be included in the final model. In fact, when this is started with connection to a simplified model of a LV grid, the significant initial transient and overshoots that manifest, make it incompatible for being integrated and simulated with MATLAB/Simulink within the simplified model of the power system that comprises the PV and the ESS plus additional three-phase AC loads.

Final and main goal of the project is to deal with proper management of the active power providing quality and reliable energy supply to these loads of a MC composed of all the elements modelled by the author and described in the previous chapters.

And this is assured via the central and fundamental element on which main focus on developing a feasible and effective control strategy has been put in this thesis: the VSC.

Of equal importance is a properly designed EMS that coordinates the contribution and the action of the two distributed power sources.

As connection to the main power system of the MG has not been considered, it is not present any analysis on how to enable operation from grid-connected mode to island mode and vice-versa.

As described In Chapter 4, stand-alone mode of operation is significantly more challenging than the grid connected mode. This because the critical demand-supply equilibrium requires the implementation of accurate load sharing mechanisms to balance sudden active power or output voltages mismatches that could cause high circulating currents.

So that the system is considered as grid-connected, either drawing or supplying power to the main grid, depending on the generation and load mix or, for instance, implemented market policies.

The block diagram and complete model of the MC are shown in Fig.66 while in Fig.67 the complete MG model created by the author with MATLAB/Simulink.

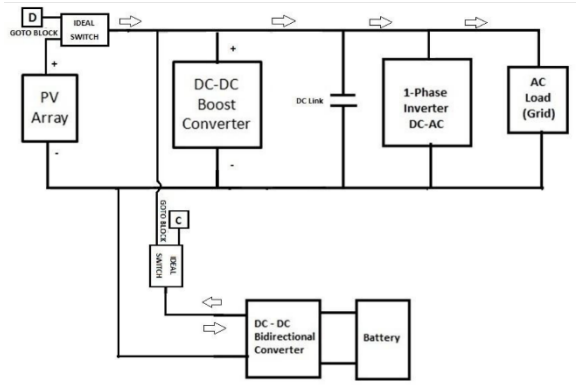

Fig. 65, Block Diagram of the proposed system, from (Sonal Gaurava, 2015)

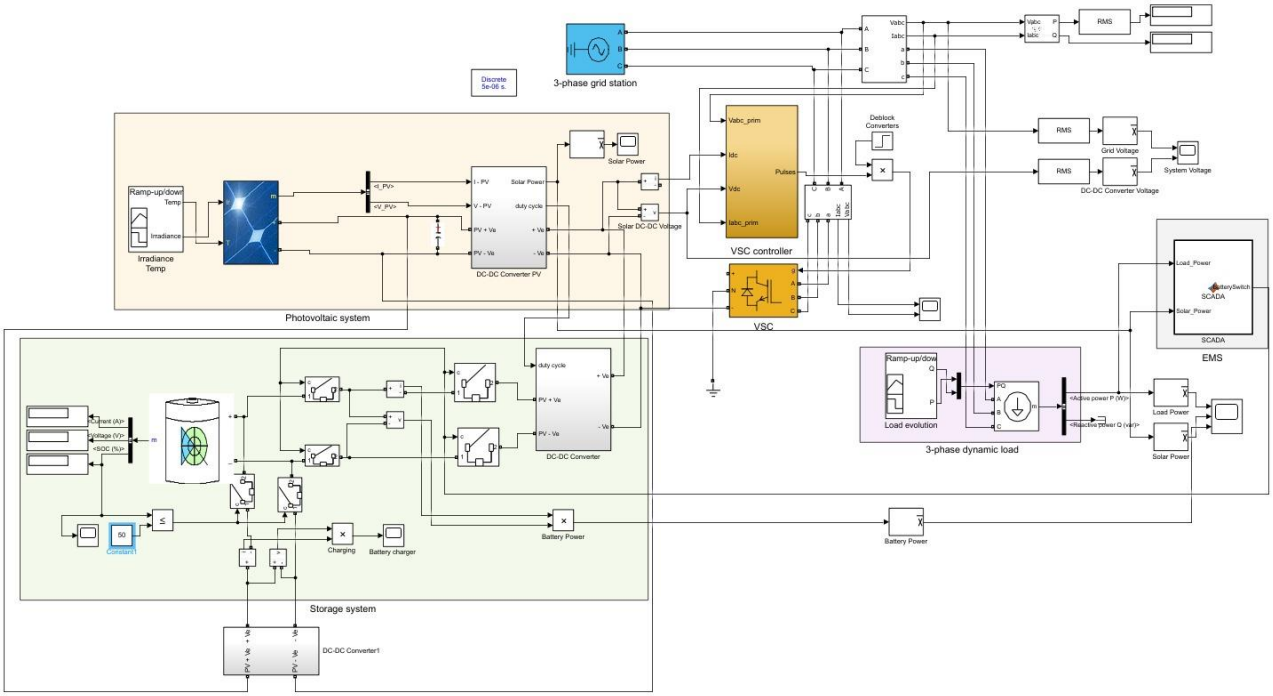

Fig. 66, Complete model of the MG: above to the left is the PV system, down to the left the ESS, in the middle in yellow the VSC controller block and the actual VSC (that consists of a 3-level full bridge) and to the right the dynamic three-phase loads and the EMS block

Depending on the requirement of the load a simplified EMS that coordinates the interaction between the ESS and the solar system, it is added. In real power systems this consists of a system of computer-aided tools used by operators of electric utility grids to monitor, control, and optimize the performance of the generation

or transmission system. To comply with such tasks and for the scope of this project an intuitive and simple MATLAB function is utilized.

```
function BatterySwitch  = SCADA(Load_Power, Solar_Power)
persistent LP SolarP BatterySwitchOld;
if isempty(LP)
    BatterySwitchOld =0;
end
if isempty(SolarP)
    BatterySwitchOld =1;
end
if Load_Power > Solar_Power
    BatterySwitch=1;
elseif Load_Power < Solar_Power
    BatterySwitch=0;
else
    BatterySwitch=BatterySwitchOld;
end
LP = Load_Power;
SolarP = Solar_Power;
BatterySwitchOld=BatterySwitch;
```

Fig. 67, Code for the SCADA/EMS system, created with MATLAB

The whole work consists of several approaches and steps and the following procedure is implemented:

- The DC voltage outputs of the PV array and the battery are input to the DC/DC converters (one for each source) that maximize the power extraction from them. The outputs from the converters is a square wave and it is necessary to convert this to a sinusoidal wave with appropriate frequency
- For this, the accumulated and combined DC power of both the sources is sent to the VSC for conversion and electrical synchronization with the distribution system
- As part of the controller of the VSC, a PLL is utilized to maintain a constant reference voltage while the control strategy is implemented in stationary frame
- From the controller we get the gating signal for the Switching device of the converter (that consists of a three-level bridge)
- the ESS is connected with the PV system using another DC-DC bidirectional converter: the SCADA system assures that breakers open and close depending if power load is greater or less than solar power activating the charging/discharging process of the battery depending even on the state of charge (SOC) of this. This is done iteratively in a closed loop cycle.
- When battery is charging from the PV system the main grid station provides power to meet the load requirement. However, when the load is not higher than solar production and battery is fully charged, the excess of solar power is uploaded and absorbed by the main grid station.

The PV array along with the battery and loads are simulated for various conditions such as:

- PV supplying the load and charging the battery
- PV supplying only the load
- PV and battery both supplying the load

So that input of irradiance for the PV array (temperature is kept to the standard condition at 25°C), sizing of the ESS and values of the three-phase loads (only active power has been considered for simplicity) are thought as to be able to simulate the different operation modes listed above.

Although a complete study for a correct sizing of both the battery and the DC/DC converter is out of scope of the project, the ESS is sized to have a rated capacity of $900\ Ah$.

For the load a maximum value of $1.7\ MW$ of active power demand has been considered. This could be compared in the order of magnitude to a residential block of a just a few hundreds of apartments (between about 200 to 400) or a large industrial facility (InfoGrid, 2012).

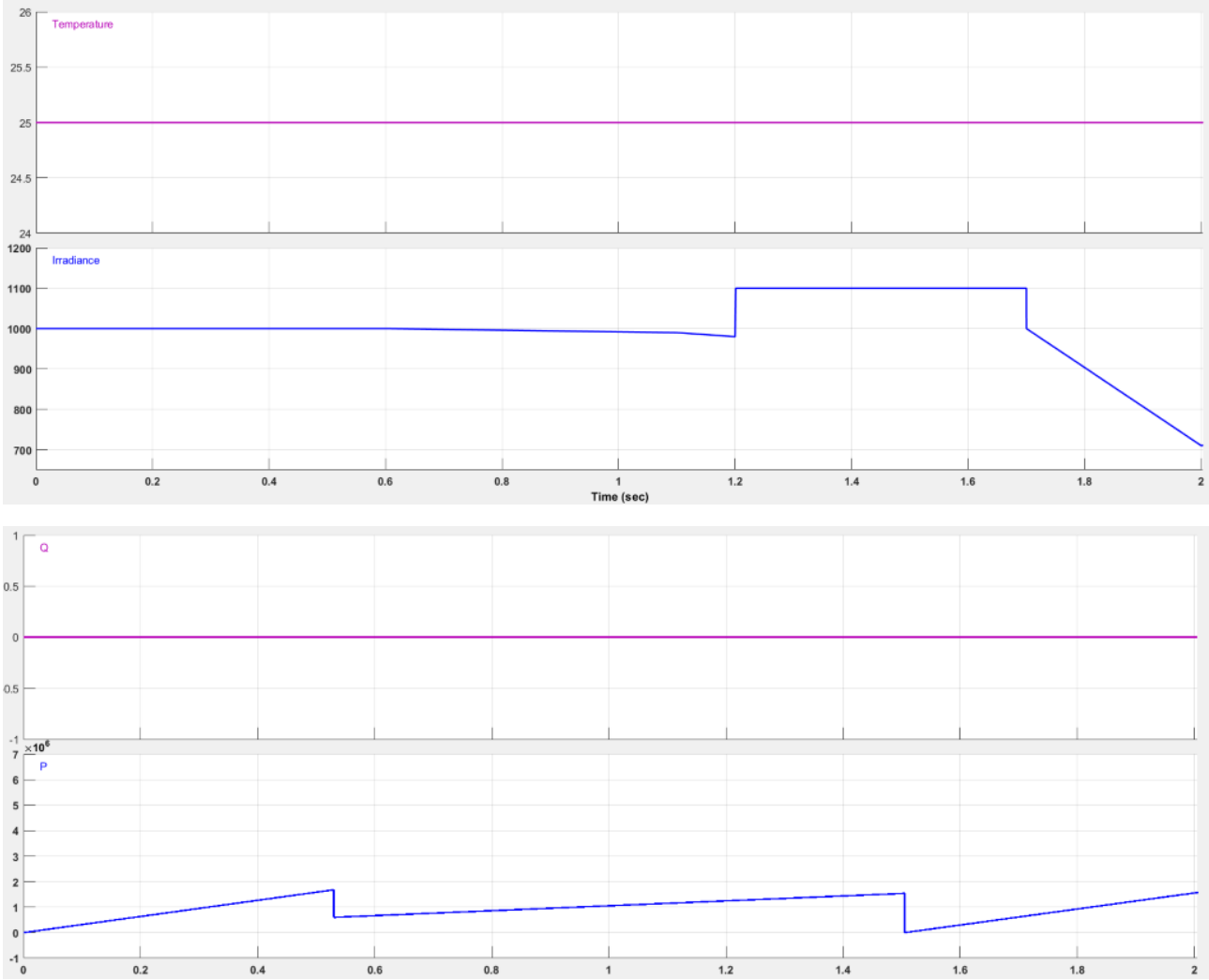

Fig. 68, Input parameters for the irradiance Ir, Temperature T and active power load P created with Simulink Signal Builder block

The significant parameters for the discussed microgrid are plotted using MATLAB/Simulink and analyzed for a simulation setup run for 2 seconds. As already mentioned, main goal is to control the battery and maximize the performance of the system by reducing the consumption from power grid by using available power from the solar panels.

7.2 Simulation

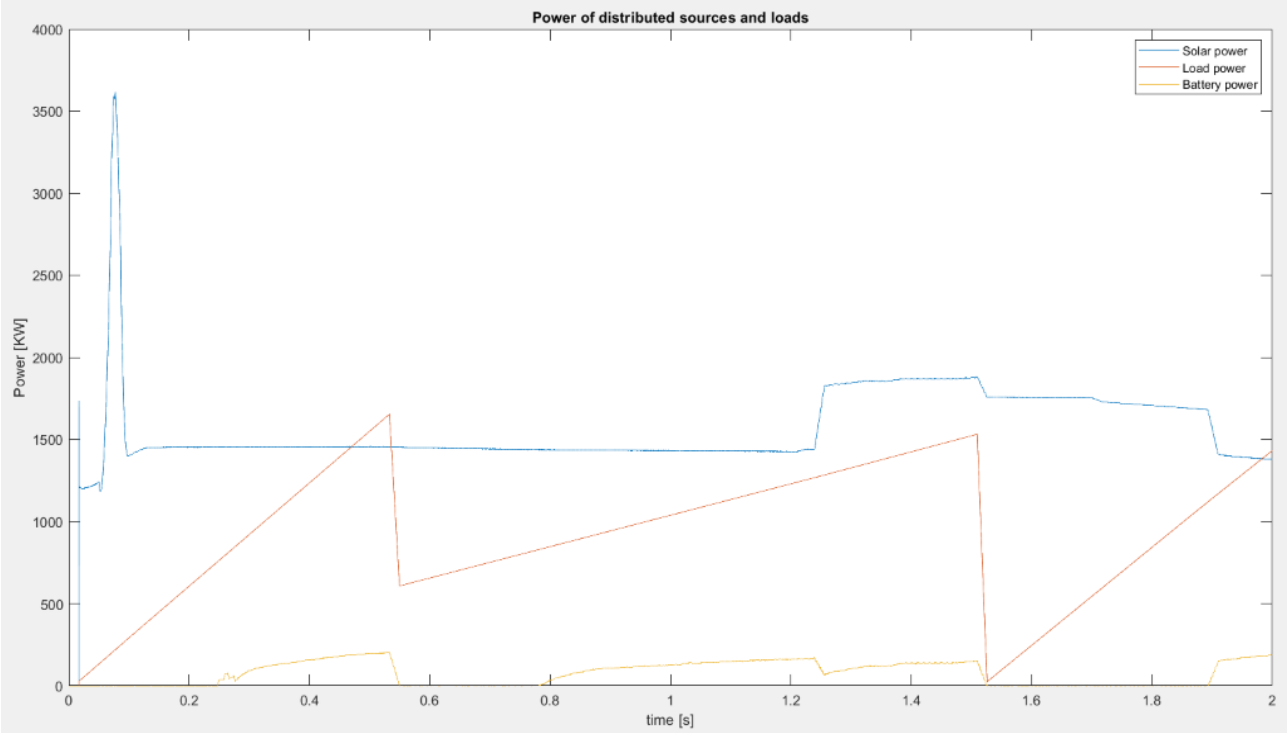

Fig. 69, Solar, battery and load power, obtained with MATLAB/Simulink

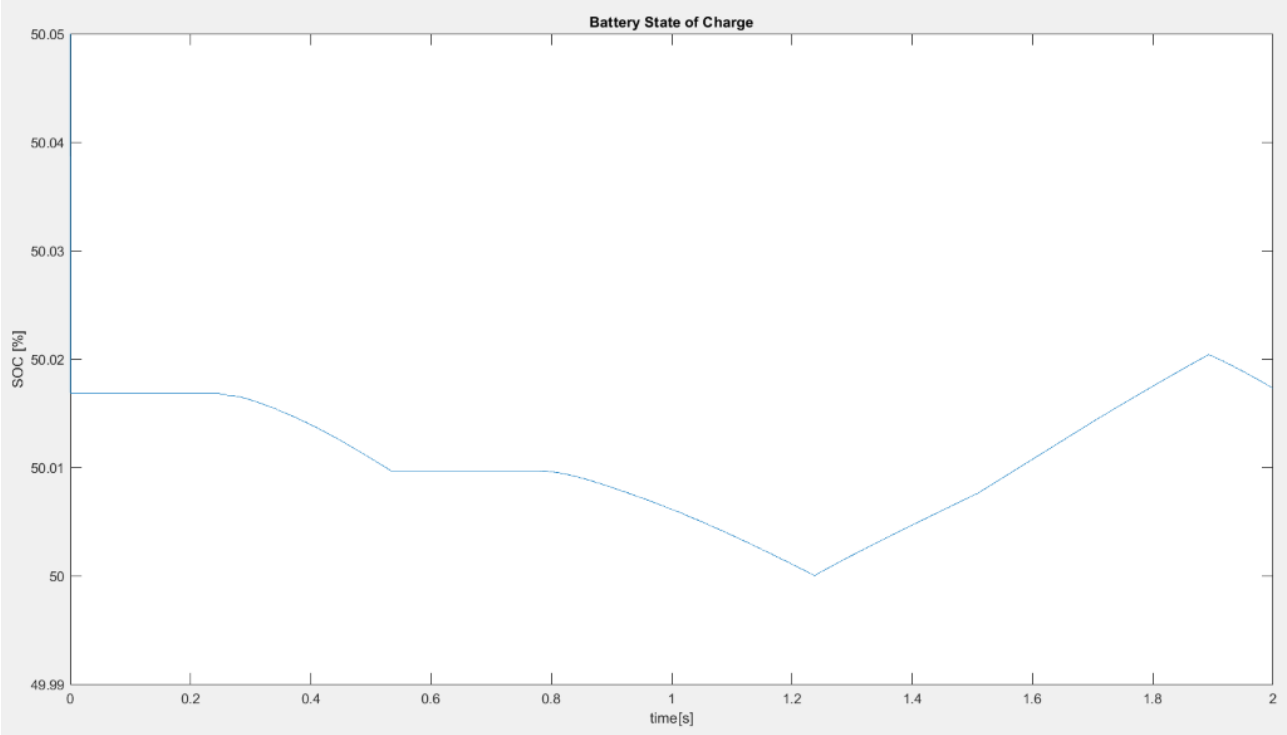

Fig. 70, Battery state of charge (SOC) profile, obtained with MATLAB/Simulink

In Fig.70, after a significant transient at the beginning of the simulation, the trend over the simulation time of the power provided by the PV system is compatible to the changing values of the irradiance input to the array. As the power demand from the load increases approaching the PV system output, battery discharging is initiated.

It can be noted that this happens before the load exceeds the power by the PV system as the controller implemented in the SCADA block is programmed to read the instantaneous power only but in the system there are abrupt fluctuations of electrical power. Controller read these fluctuations and activate the battery source operating the switches. On the other hand, the scope is programmed to display the mean values data, and that is the reason for which battery looks like it activates earlier.

In Fig.71, are displayed showing compatible and consistent results with ones obtained in Fig.70. Notice that, when the solar power output exceeds the load the state of charge of the battery decreases (battery is injecting power to the DC bus). On the other hand, when the active power consumed is well covered by the PV system output, the state of charge increases (meaning that the DC bus is supplying power to the battery, from $t = 1.25\ s$ to $t = 1.95\ s$). But this behavior manifests only when SOC of the battery approach the 50% mark (for the sake of simulation over such a short time, battery is initiated at a 50.05% of SOC so that this limit is reached quite fast due to the high transient of the solar generation). It can be observed the bidirectional behavior of the system and the need of using a DC/DC converter.

All the conditions for which PV is supplying the load and charging the battery, the PV system is exclusively supplying only the load and both the PV and the battery are supplying the load have been simulated showing proper functioning of the system.

8. Conclusions

8.1 Main Findings

This paper presented modeling and simulation of a MG in MATLAB Simulink. For simplicity purposes, this MG was treated as a grid-connected system and controlled to be able to utilize different energy sources collaborating to achieve the overall goal, which is supplying the electric load. The results were presented, showing that the renewable energy coming from the solar panels and the ESS it is optimally utilized, along with the possibility of interaction with the grid distribution system and via the deployment of the power converter as central and fundamental component of the system. Each component was treated as an autonomous system with preliminary tests before being included in the MG. As mayor difficulties were encountered by the author for the integration of the wind energy system, this has not being included so that future work in this sense is necessary.

After running the most important simulation of the designed system and displaying the most relevant results we can extract some important conclusions.

In order to simulate embedded power electronic systems is much more efficient to simulate an averaged model rather that a realistic one being less time-consuming, simpler and quicker for simulation as the used that is software presents less computational problems. Especially for the analysis of the VSC, results have proved to be accurate enough to be valid for the study of active and reactive power control.

Although the impact of varying the magnitude of the critical load on the dynamic characteristics of the MG has been investigated, in the same way, future work is also needed to investigate grid behavior more thoroughly including for instance the operation of this under unbalanced voltages and currents or introduction of harmonics.

Another important conclusion is that, as said due to the problems occurred in integrating the wind power system and not considering any additional electrical sources (for instance fossil-fuel generators or other possible back-up solutions), to cover the electrical demand with values presented in this work, the approximate total area of solar panels needed would be around 9000 m^2. This considering standard irradiance and temperature over the length of a day so that such number results quite high.

Even though, without considering the project in economic terms, the project could result technologically feasible, only considering the total amount of rooftop area available (for instance of a large commercial or industrial facility) corresponding to the magnitudes of the loads analyzed or simply better evaluating the geographic positioning of the MG.

As an accurate sizing of the storage system is not in the scope of this project and have been just partially addressed to be match with and providing assistance to the solar system in providing the electrical load, further work is necessary. This would represent an interesting way of both continuing the work done so far by the author and an opportunity to enhance knowledge of a topic that is of milestone importance for further penetration of renewable distributed sources in LV distribution systems.

8.2 Environmental impact

Much as already being said throughout the paper about the many possible benefits that the introduction of MGs could add to the whole energy industry, especially for national transmission system operator (TSO) or distribution system operator (DSO). Between these we find the improvement of the operation, stability and reliability of the regional electric grid and reduction of the grid "congestion" and peak loads. This helps to delay investments on new electric infrastructures.

But from an environmental point of view, it is the ability to be particularly apt to integrate RERs into the power system that represents the main asset of MC. So that, along the many other advantages just mentioned, thanks to this it is possible to provide efficient, low-cost, clean energy (reducing the amount of the annual GHG emissions), to enhance energy efficiency and to foster sustainable energy development (that became a priority for many countries all over the globe).

As it will be discussed in this section, MG configuration with the incorporation of renewable energy resources and electric storage system has an impact not only in economic terms (considered to be positive by both the papers cited in this paragraph) but in environmental term as well.

That is, the amount of gaseous pollutants released into the atmosphere for production of power is significantly reduced when not using traditional power plants and transmission/distribution systems for providing electrical power.

In (Bansalb, 2018) the objective of the research work is to minimize the cost of energy, the annual cost of load loss and the lifecycle greenhouse gas emission cost to improve the overall benefit of green technologies in the proposed MG system. The suitability of the proposed model is tested on six case studies by using the same load profile, wind speed and irradiation of the site and diesel generator power capacity. These cases range from a first scenario where the diesel generator is designed in such a way to meet the load demand of the consumers since no other power source is available, to the last one where the integration of the additional number of PV generators, wind turbine generators (WTG) and ESS units into the proposed MG system entirely replaces the power output contribution of the diesel generator.

The PV and WTG are reported to be the most popular renewable distributed energy resources based on the availability, affordability, protection of the environment and for being cheaper than other low-emission technologies, clean energy options.

The results obtained, besides demonstrating the optimal feasibility of renewable energy resources in a MG system, show a significant reduction in the values greenhouse gas emission when compared with case study 1, shows that the utilization of green technologies in a MG system optimizes the environmental impact.

With an analysis made over a time horizon of 25 years the integration of the additional number of the PV, WTG and ESS units into the proposed MG system allows to save the lifecycle quantity of Carbon dioxide (CO2), Nitrogen oxide (NOx) and Sulphur dioxide (SO2) emissions of $1.39 \times 10^3\ ton$, $1.39\ ton$ and $0.761\ ton$ respectively.

In (Ali, 2017) a rural area with some decades of households is considered. This has no resources for building the large utility for electricity supply, hence, it relies entirely on the national grid for electricity supply.

Aiming to cut down the electricity loss due to transmission line, and by utilizing the renewable energy to supply energy to this area, a MC, consisting of a $32\ kW$ micro-wind power plant and a $10\ kW$ PV power plant, is planned to be installed and studied.

Results obtained show once again significant reduction of the amount of gaseous pollutants released into the atmosphere when comparing different options in supplying electricity to the community. According to the local Electric Power Company, the CO2 emission intensity of power supplied by the utility grid is $0.381 Kg/kWh$ while, for micro-wind power plants and solar power plants, they are $0.0295 Kg/kWh$ and $0.072 kg/kWh$ and this emission intensity figures are based on an accurate life cycle analysis which incorporates the emissions from construction, operation, dismantling and disposal of the power sources that have been taken into account.

From the final result, it is show that the total amount of CO2 emission will be reduce a total of $8\ ton$ for an average one month when the load takes most of its energy supply from the renewable MG model studied. Once again, this is indeed a worth noting environmental impact.

For concluding this section, the concept of net-zero energy community (ZEC) or net-zero energy building (ZEB) is introduced. A building or community with zero net energy consumption means that the total amount of energy used by these on an annual basis is equal to the amount of renewable energy created on the site, or in other definitions by renewable energy sources offsite (Wikipedia, Zero-energy Building).

This is of particular interest as in (Nancy Carlisle, 2009) a particular classification system where, for instance, a community that offsets all of its energy use from renewables available within the community built environment and redeveloped sites is considered at the top of it for minimizing its environmental impact.

Energy is the primary focus of (Nancy Carlisle, 2009), but when developing a net-zero energy solution, one needs to be mindful that a successful solution must be one that works in terms of energy as well as other parameters of sustainability. For example, intentionally building low-density buildings to maximize roof area for PV, which results in increased traffic and limits access to community amenities for certain populations without access to cars, would not be considered in keeping with the principles of sustainability.

So that, even though an accurate analysis of neither the geographical positioning nor the design and layout of buildings that would compose the MG model object of this work, some interesting conclusions have already been stated in this chapter: the project showed technological feasibility, taking into account rooftop area potentially available even in a prebuilt residential or industrial environment, without the necessity of utilizing green space within the community or located outside the community boundary.

Besides this, assuming that the community is grid connected, as it has been considered in this work, the net-zero concept allows this to go into a carbon electricity debt through the winter months and “break even” at the end of the summer season with excess PV generation.

Taking into account the mentioned aspects, the specific model of MG developed by the author with its load and sources characteristics it is likely to be positively ranked in the classification system proposed by the cited paper.

In this section it is made clear how environmental impact is significantly reduced when using renewable energy resources integrated MC instead of traditional power generation and distribution methods, and therefore how necessary it is to change the pattern of energy consumption from heavily depending on fossil-fuels to cleaner alternatives. Worth noting that the electricity power sector accounts for a significant proportion of overall global emissions that are cause of global warming and greenhouse effect.

8.3 Project cost

This section is meant to summarize the monetary and time costs. Direct costs are linked to the work carried out on the project, such as for example project materials or direct labor.

In order to be able to make this project, it is mandatory to buy one of the latest versions of the MATLAB software with Simulink included. The cost of such license is of $2000€$ but it is not been considered in the final calculation of the cost since it is made available free of charge by the UPC for each student. So that the lion's share of it consists only of the time being investment into the project.

The approximated time needed is on the order of an entire semester of regular work, including the documentation process and literature review, contacting the coordinator of the thesis project to set up regular meetings and eventually the actual developing of the work.

This project revealed to be quite time consuming, mainly because of the many difficulties encountered in making the final model of the MG working correctly using the software, and the thirty credits of twenty-five hours each, estimated as necessary to complete the project, which in turn add up to a total of five hundred hours, so that this is not too far off the mark in this case.

So that taking into account a standard hourly salary of $7.5€/h$ for a master student employed as intern a straightforward estimation can be done for the total cost of the project that sums up to $3750€$.

Bibliography

Adam Hirscha, Y. P. (2018). *Microgrids: A review of technologies, key drivers and outstanding issues.*

Agust Egea-Alvarez, A. J.-F.-B. (2012). *Active and reactive Power control of grid connected DG Systems.*

Ahmed, K. A. (2010). *Modeling and Simulation of PV Array.*

Ali, Z. Z. (2017). *Economic and Environmental Impact Assessment of Microgrid for Rural Areas of Pakistan.*

Bansalb, T. A. (2018). *Reliability, economic and environmental analysis of a MG system in the presence of renewable energy resources.*

Bilal Mouneir, N. A. (2014). *Control Methods and Objectives for Electronically Coupled Distributed Energy Resources in Microgrids: A Review.*

C. K. Sao and P. W. Lehn, ". a. (2008). *Control and power management of converter fed microgrids.*

Cantarellas, A. M. (Jan. 2018). Competitive power control of distributed power plants.

Daniel E. Olivares, A. M.-S.-B. (2014). *Trends in Microgrid Control.*

El-Saadany, M. F. (2012). *Incorporating DFIG Based Wind Power Generation in Microgrid Frequency Regulation.*

F. Blaabjerg, R. T. (2006). *Overview of control and grid synchronization for distributed power generation systems.*

G. Abad, J. L. (2011). Back-to-Back Power Electronic Converter. In J. L. G. Abad, *'Doubly Fed Induction Machine: Modeling and Control for Wind Energy Generation.*

G. Abad, J. L. (2011). Introduction to A Wind Energy Generation System. In J. L. G. Abad, *Doubly Fed Induction Machine: Modeling and Control for Wind Energy Generation.*

Green, M. P. (2006). *High-quality power generation through distributed control of a power park microgrid.*

He, J. H. (2008). *Modeling and control of grid-connected voltage-sourced converters under generalized unbalanced operation conditions.*

He, J. H. (2008). *Modeling and control of grid-connected voltage-sourced converters under generalized unbalanced operation conditions.*

InfoGrid, U. R. (2012). *What is a Megawatt?* Retrieved from http://www.utilipoint.com/2003/06/what-is-a-megawatt/

Iravani, A. T. (2008). *Multivariable Dynamic Model and Robust Control of a Voltage-Source Converter for Power System Applications.*

Iwanski, G. A. (2014). Properties and Control of a Doubly Fed Induction Machine. In G. A. Iwanski, *Power Electronics for Renewable Energy Systems: Transportation and Industrial Applications.*

Joan Rocabert, A. L. (2012). *Control of Power Converters in AC microgrids.*

José Rodríguez, S. M. (2007). *Predictive Current Control of a Voltage Source Inverter*.

K. D. Brabandere, B. B. (2007). *A voltage and frequency droop control method forparallel inverters.*

Kao, Y. W.-N. (2009). *] An Accurate Power Control Strategy for Power-Electronics-Interfaced Distributed Generation Units Operating in a Low-Voltage Multibus Microgrid.*

Laboratory, N. R. (2017). *Microgrid-Ready Solar PV.*

Li, Y. L. (2011). *Power management of inverter interfaced autonomous microgrid based on virtual frequency-voltage frame.*

Marola, A.-M. (2020, Jan. 3). *Share of renewables in energy consumption in the EU reached 18% in 2018.* Retrieved from https://ec.europa.eu/eurostat/web/energy/overview

Muhammad Yaqoob, J. A. (2019). *A Comprehensive Review on a PV Based System to Harvest Maximum Power.*

Nam, H.-s. S. (2009). *Dual Current Control Scheme for PWM Converter Under Unbalanced Input Voltage Conditions.*

Nam, H.-s. S. (2011). *Dual Current Control Scheme for PWM Converter Under Unbalanced Input Voltage Conditions.*

Nancy Carlisle, A. O. (2009). *Definition of a "Zero Net Energy" Community November.*

Nee., L. H.-P. (1998). *Model-based current control of ac machines using the internal model control method.*

Nee., L. H.-P. (1998). *Model-based current control of ac machines using the internal model control method.*

Snehamoy Dhar, R. S. (2015). *Modeling and Simulation of PV Arrays.*

Sonal Gaurava, C. B. (2015). *Energy Management of PV - Battery based MG System.*

Toshihiko Noguchi, H. T. (1998). *Direct Power Control of PWM Converter Without Power-Source Voltage Sensors.*

Units F. Katiraei, M. a. (2009). *Power Management Strategies for a Microgrid With Multiple Distributed Generation.*

Wikipedia. (n.d.). *Direct-quadrature-zero transformation.* Retrieved from https://en.wikipedia.org/wiki/Direct-quadrature-zero_transformation

Wikipedia. (n.d.). *HVDC converter.* Retrieved from Wikipedia: https://en.wikipedia.org/wiki/HVDC_converter

Wikipedia. (n.d.). *Solar cell*. Retrieved from Wikipedia: https://en.wikipedia.org/wiki/Solar_cell

Wikipedia. (n.d.). *Zero-energy Building.* Retrieved from Wikipedia: https://en.wikipedia.org/wiki/Zero-energy_building

WindPower, B. (2019). *Small Wind Turbines for Microgrids.*

Yasser Abdel-Rady Ibrahim Mohamed, E. F.-S. (2008). *Adaptive Decentralized Droop Controller to Preserve Power Sharing Stability of Paralleled Inverters in Distributed Generation Microgrids.*